Journal of Environmental Chemical Engineering xxx (xxxx) xxx–xxx

Contents lists available at ScienceDirect

Journal of Environmental Chemical Engineering

journal homepage: www.elsevier.com/locate/jece

A review of integrated photocatalyst adsorbents for wastewater treatment

N. Yahya[a,b], F. Aziz[a,b,*], N.A. Jamaludin[a,b], M. A. Mutalib[c], A.F. Ismail[a,b], W.N. W. Salleh[a,b], J. Jaafar[a,b], N. Yusof[a,b], N. A. Ludin[c]

[a] Advanced Membrane Technology Research Centre (AMTEC), Universiti Teknologi Malaysia, 81310, UTM Johor Bahru, Johor, Malaysia
[b] Faculty of Chemical and Energy Engineering, Universiti Teknologi Malaysia, 81310, UTM Johor Bahru, Johor, Malaysia
[c] Solar Energy Research Institute (SERI), Universiti Kebangsaan Malaysia (UKM), 43600 Bangi, Selangor, Malaysia

ARTICLE INFO

Keywords:
Photocatalyst
Adsorbents
Wastewater
Perovskite
Integrated photocatalyst adsorbents

ABSTRACT

Photocatalysis has the best potential to replace the conventional wastewater treatment technology due to its utilization of visible light to photo-degrade organic and inorganic contaminants. However, when applied in slurry form, agglomeration of nanoparticle will lead to serious decrease in photocatalytic performance due to hinderance effect. By combining the photocatalyst and adsorbents, which is designated as integrated photocatalyst adsorbent (IPCA), an adsorbent material which also degrades toxic organic compounds in the presence of UV/visible light irradiation could be produced. The compound does not only preserve all the interesting characteristics of both individual components, but also overcomes serious drawbacks, such as low absorptivity, rapid recombination of photogenerated electrons and hinderance effect of photocatalyst when applied in slurry form. There are several criteria that must be obeyed by the absorbent material used such as high absorption capacity to target compound, reasonable transparency to UV–vis light, high surface area, inhibition of photocatalyst leaching and good stability with dispersing solvent. In this review article, the authors presented an overview on the application of photocatalyst, adsorbents and integrated photocatalyst adsorbents for wastewater treatment. Moreover, the discussions were also focused on the major adsorbent which has been integrated with photocatalyst such as carbon, clays, zeolite matrix materials and others. Additionally, the mechanisms of the adsorption of emerging organic contaminants with adsorbents in IPCA were also discussed to clearly understand the possible interactions between organic contaminants and IPCA. Outlook on IPCA study were also discussed to further broaden the prospective of this technology.

1. Introduction

Water is a precious source that is important to every living thing throughout the world. Water covered almost 70 percent on the earth but only 2.5% is indicated as clean water. The minor amount of clean water is used, recycled, and then treated so that it can be repurpose again. Usage of water is not only limited to domestic usage but also in broad areas of application including industrial and agriculture. According to UN WWAP in 2003, about 2 million tons of untreated water originates from industrial and agriculture water runoff. Increased amount of water usage would generate increased amount of wastewater. Wastewater treatment requires high cost because the contaminant present in the wastewater must be removed effectively so that water can be reuse again safely. Even with conventional methods such as biological and physical treatments, to remove the contaminants effectively would still require more advanced technology with lower cost and shorter time requirements [1]. Thus, findings the best practices/strategies for wastewater management are crucial for our environment and sustainable development.

Nowadays, various kind of materials have been employed to remove the contaminants from wastewater, including catalyst (homogenous and heterogenous), adsorbents, membrane from organic and inorganic materials, ozone, etc [2–7]. The conventional water treatment technologies that are available nowadays such as adsorption or coagulation, does not completely eliminate or destroy the pollutants. Somehow, these pollutants were simply being concentrated by transferring them another phase. Hence, finding an alternative water treatment technology that can completely eliminate or destroy these contaminants is highly sought after. Advanced oxidation processes (AOPs) is a recently discovered wastewater treatment technology which treats pollutants by generating hydroxyl radicals which are responsible for organic degradation. Due to their strong unselective oxidative power, the hydroxyl radicals oxidize and mineralize almost any organic molecule, yielding CO_2 and inorganic ions as final products [8]. The generation of

* Corresponding author at: Advanced Membrane Technology Research Centre (AMTEC), Universiti Teknologi Malaysia, 81310, UTM Johor Bahru, Johor, Malaysia.
E-mail addresses: farhanaaziz@utm.my, farhana@petroleum.utm.my (F. Aziz).

https://doi.org/10.1016/j.jece.2018.06.051
Received 18 April 2018; Received in revised form 6 June 2018; Accepted 23 June 2018

hydroxyl radicals can be initiated by primary oxidants (hydrogen peroxide, ozone), energy sources (UV light, ultrasonic and heat) or catalysts (titania, zinc oxide and Fenton reagent) [9]. Among AOPs, photocatalysis is an interesting alternative process that can remove the emerging contaminants at ambient temperature and pressure by oxidation.

Various semiconductors have been applied as photocatalysts for photo-degradation of organic and inorganic contaminants [10]. Amongst them, titanium dioxide (TiO_2) is the most widely studied since it is non-toxic, chemically stable, commercially available and inexpensive [4,8]. However, the practical applications of photocatalytic TiO_2 have been hindered due to its intrinsic properties such as low quantum yield and wide band gap (3.2 eV), which limits the utilization of TiO_2 in visible-light [4,8]. To enhance the solar efficiency of photocatalyst under solar radiation, it is necessary to modify the nanomaterial to facilitate visible light absorption. Non-metal and transition metal doping is one of the strategies used to narrow the band gap of TiO_2 to activate them under visible light or direct sunlight irradiation. Besides, many studies have been focused on designing and developing on the single-phase oxide photocatalyst such as perovskite-type oxide materials working under visible light illumination [6,9].

Adsorption technology which categorized under physical techniques are one of the promising treatment options for pollutant removal due to its efficiency, simplicity, inexpensive and unaffected by toxicity [11,12]. When solely utilized, this method is unable to completely eliminate or destroy the pollutants, but rather concentrates the pollutants through absorption and separates it from the system. Various adsorbents have been reported in published works for the removal of pollutants such as activated carbon, clays, zeolite, and polymeric adsorbents [13–16]. Activated carbon has been a material of choice for several pollutants in an adsorption-based removal process. Graphene oxide (GO) is regarded as a single layer carbon based material which contains abundant oxygen-containing functional groups, has attracted considerable attention over the years due to its excellent physicochemical and mechanical properties [17,18]. Graphene has been widely applied as an adsorbent for wastewater treatment due to its excellent adsorption capacity for organic pollutant [18–20].

The main drawback of photocatalyst nanoparticles is when applied in slurry form, agglomeration of nanoparticles will lead to serious decrease in photocatalytic performance [21–24]. Non-porous and polar surface of the photocatalyst will also cause a decrease in the adsorption of the pollutants on its surface, thus reducing the photodegradation rate. To overcome this, recent studies have focused on immobilizing the photocatalyst on adsorbents such as carbon, clays, zeolite and others. By combining the photocatalyst and adsorbents, which is designated as integrated photocatalyst adsorbent (IPCA), an adsorbent material which also degrades toxic organic compounds in the presence of UV/visible light irradiation could be produced [25]. This synergistic combination does not only preserves all of the interesting characteristics of both individual components, but also overcomes serious drawbacks, such as low absorptivity and rapid recombination of photogenerated electrons [26]. Immobilizing photocatalyst on adsorbents materials is favourable compared to in slurry form as this will ease the separation of IPCA from bulk solution for reusing the photocatalyst.

The research on integrating the photocatalyst with adsorbents has started way back in 1999 when Burns and his co-workers proposed a fouling prevention strategies for TiO_2 catalyst [27]. Motivated from their success, a lot of works in IPCA has been conducted and degradation/performance as high 98% for 18 min under visible light irradiation has been observed [28]. Surprisingly, limited number of studies has been performed in this area. Thus, the aim of this review is to critically summarize the major works regarding the removal of emerging organic contaminants from wastewaters using photocatalyst, adsorbents and integrated photocatalyst adsorbents (IPCA). The available methods to prepare doping solution of TiO_2 and significant factors that affects the properties and performance of TiO_2 doping were extensively discussed. Besides, the discussions were also focused on the major adsorbent used that has been integrated with photocatalyst which include carbon, clays, zeolite matrix materials and others. Additionally, the mechanisms of the adsorption of emerging organic contaminants with adsorbents in IPCA were also stated to clearly understand the possible interactions between organic contaminants and IPCA.

2. Photocatalyst

Photocatalyst has found its way since in 1972 by Fujishima and Honda when they had discovered Titanium Dioxide (TiO_2). During at that time, the purpose of TiO_2 was for water splitting into hydrogen and oxygen in a photo-5 electrochemical cell. This discovery has propagated researchers to explore the usage of TiO_2 in many areas especially in photocatalysis. One of the earlier works on photocatalysis for wastewater treatment was conducted by Bahnemann and co-workers in 1991 using TiO_2 suspensions [29]. They reported on the influence of light intensity, temperature and pH on the degradation rate of halogenated hydrocarbons using TiO_2 photocatalyst suspensions. They have concluded that this technology has a bright potential for wastewater treatment applications and detailed study are needed to further develop this technology. Inspired from this, a lot of research work has been conducted by using TiO_2 as photocatalyst.

2.1. Titanium dioxide (TiO_2) and doped-TiO_2

To pick the right and suitable photocatalyst, one must give attention to the band gap value. Usually semiconductors are preferred to act as photocatalyst because the narrow band gap, particularly between 1.4–3.8 eV [1]. TiO_2 has many reason to become one of the most suitable photocatalyst such as low-cost, high chemical stability, commercially available, non-toxic, and environmental friendly [2,3]. The major drawback of TiO_2 as photocatalyst is the wide band gap. The band gap of this material limits the absorption of only small portion of the solar spectrum (UV region) [4]. Yu et al. (2011) studied the degaradation of bacterials, and found that TiO_2 is a good phototcatalyst but lack the visible light utilization that cause low quantum yield [5]. Absorption in normal sunlight is limited due to the large and wide bandgap (3.2 eV) [6]. Larger band gap would require higher energy to activate the photocatalyst while TiO_2 only offer the absorption wavelength of less than 400 nm. Due to this major drawbacks, researcher has found many ways to overcome the drawbacks including non-metal and transition metal doping as listed in Table 1.

It is known that the methods used to prepare doped TiO_2 solution have significant impact on the catalytic properties and performances. There are many methods available to prepare doped TiO_2 such as sol-gel, hydrothermal hydrolysis, co-precipitation and many more [30,43]. One of the common methods to synthesis doped TiO_2 solution is sol-gel procedure. This method uses simple instruments and simple procedure in preparing the nanomaterials. Since mid-1800s, sol-gel technology has been applied in many applications such as membrane, catalysis, chemical sensors, etc [44]. Zhou et al. [35] synthesized Vanadium-doped TiO_2 via sol-gel method and added Ti $(OBu)_4$ as a precursor to measure methyl orange degradation [35]. In 2012, Li and Wen synthesized Lanthanum-doped TiO_2 by using sol gel method combined with supercritical fluid drying (SCFD) method. The combination of both methods producing uniform small size of crystal [21].

Other than sol-gel method, hydrothermal method is another option to prepare doped TiO_2. Single doped of Yttrium (Y) with TiO_2 has been synthesized by Khan and Cao [41] via hydrothermal method. Uniform size of crystal were produced with reduction in band gap, which consequently enhancing the photocatalytic activity under visible light irridiation. Khalid et al. [37] prepared Carbon-Yitrium-co-doped with TiO_2 via hydrothermal method and observed an increment in photocatalytic activity of doped and co-doped samples due to smaller

Table 1
TiO_2 doping to narrow band gaps.

Non-metal/ transition metal doping	Band gaps (eV)	Significant findings	References
Ferum(III) ions-doped TiO_2	2.99	Value of eV decreasing with the increasing amount of doped content	[30]
Chromium(III) ions-doped TiO_2	3.33	Value of eV decreasing with the increasing amount of doped content	[30]
Sulphur-doped TiO_2	–	Performance rate of degradation of methylene blue for doped TiO_2 maintain high under irradiation at wavelength longer than 440 nm compare to pure TiO_2	[31]
Antimony(Sb)-doped TiO_2	–	100 ppm of methylene blue could be decomposed within one hour by using 5% of Sb-doped TiO_2.	[32]
Ferum-ion-doped TiO_2	–	0.09% Ferum(III) ions and Fe(II) ions doped TiO_2 exhibited high photocatalytic activity toward degradation of XRG dye compared to undoped TiO_2	[33]
Lantthanum-Nitrogen-co-doped TiO_2	–	Decomposition of methyl orange is completed within one hour at concentration of 0.5 atomic% and temperature of 550 °C.	[34]
Vanadium(V)-doped TiO_2	–	Absorption threshold is red shifted from 380 nm to 650 nm.	[35]
Lanthanum-doped TiO_2	–	Optimum value concentration of dopant in this study is 0.02 mol % La-TiO_2 and improved by 30.7% than pure TiO_2 for photocatalytic activity.	[36]
Carbon-Yitrium-co-doped TiO_2	–	Carbon-Yitrium-co-doped TiO_2 showed highest absorbance value which is 405 nm compared to single doped and pure TiO_2.	[37]
Zinc-doped TiO_2	–	Degradation of nitrobenzene by using Zinc-doped TiO_2 showed 99% compared to pure TiO_2 which only 70%.	[38]
Chromium(III) ions-doped TiO_2	–	Optimum values concentration of dopants are 0.15% and 0.12% under UV light and visible light toward degradation of XRG dyes and improved photocatalytic activity than pure TiO_2.	[39]
Cerium dioxide-doped TiO_2	3.15	Band gap reduced from 3.29 eV to 3.15 eV.	[40]
Yttrium(Y)-doped TiO_2	1.94	Yttrium(Y)-doped TiO_2 enhanced photocatalytic activity than pure TiO_2, showed decreasing value of band gap and improved separation of electron-hole pairs	[41]
Nitrogen-doped TiO_2	–	Nitrogen-doped TiO_2 showed higher photocatalytic activity under visible irradiation towards azo dye Orange G (OG) compared to TiO_2.	[42]

crystallite size and enhanced visible light absorption.

Co-precipitation method also can be applied in preparing doped TiO_2. Zuas et al. n.d, [40] have synthesized cerium dioxide (CeO_2) by using co-precipitation method and they observed that the catalyst has lower the band gap value from 3.29 eV to 3.15 eV. Antimony(Sb) doped TiO_2 also been synthesized via the same method and current procedure exhibited uniform texture of dopants and thus formed stable solid solutions with TiO_2 [32]. Co-precipitation also can be seen as a potential method to be applied in large scale. Quan et al. (2007) made a comparison between sol-gel method and co-precipitation method by using Lanthanum-doped TiO_2 toward effectiveness of photocatalytic activity. Based on the result, co-precipitation method produced higher photocatalytic activity than sol-gel method.

Interestingly, recent study have combined hydrothermal method with another method. Zhu et al. [45] sythesized Chromium (III) ions (Cr^{3+}) doped TiO_2 by combined hydrothermal method and sol-gel method. Both of the methods are essentail as they contribute respective benefits in the dopant solution. For sol-gel method, it assists on the bulk trap and transmission of charge carrier while for hydrothermal method, it promotes dopant transitional metal distribution in TiO_2 and to prevent from heteregenous metal oxides phases [45].

Few factors have been proved to have significant effects toward enhancing photocatalytic activity. One of them is level of dopant concentration. Dopant concentration effect would cause an increase in the photocatalytic activity and thus, increase the efficiency of degradation toward pollutants. Earlier works in TiO_2 doping conducted by Moon et al in 2001 regarding the concentration of dopant in Antimony(Sb)-doped TiO_2 and the result showed the increasing doping concentrations from 1 to 5%, had increased photocatalytic activity toward degradation of 100 ppm of Methylene blue [32].

Vanadium-doped TiO_2 prepared by Zhou et al. [35], also discovered that the concentration of dopants influenced the photocatalytic activity, in which higher concentration of dopant ions will lead to a narrower band gap [35]. Malengreaux et.al prepared single doped Fe^{3+} and Cr^{3+} and discovered that by increasing the content of dopants, it resulted in the narrowing the band gap [30]. On the other hand, a study by Q. Li and Wen in 2012 stated that instead of increasing content of dopants, optimum value of concentration of dopant is important to enhance the photocatalytic activity. Based on the study, smaller concentration cannot enhance while excessive concentration will eventually reduce the photocatalytic activity. Increasing dopants to above 5% will lead to the reduction in photocatalytic activity [30].

Other than the concentration of dopants, calcination temperature can also influence the photocatalytic activity by presence of anatase structure. Ohno et al. [31] studied calcination temperature effect on sulfur doping with TiO_2. Calcination temperature at 500 °C was found to be the optimum temperature at which the strongest photo absorption occurs in visible area compared to temperature at 400 °C, 600 °C and 700 °C. Above 500 °C, the anatase composition was reduced and promoted to rutile phase. On the other hand, further study regarding to effect of calcination temperature on carbon doping with TiO_2 revealed that 400 °C is the optimum temperature for the photocatalytic activity as the XRD result showed anatase peak appeared at that particular temperature and peak of anatase is begin to decrease above 400 °C [46].

The presence of certain elements in doping also can influence the photocatalytic activity. Wei et al. [34] discovered that the presence of Lanthanum element in Lanthanum-Nitrogen-co-doped TiO_2 can prevent the aggregation of powder when it was calcined at high temperature in the presence of Nitrogen. Additionally, the band gap was also narrowed. For co-doped cases with TiO_2 that contains La^{3+} - Fe^{3+} and Eu^{3+}- Fe^{3+}, values of band gap is influenced by the presence of Ferum (III) ions [47]. Zhu et al. [45] used $FeCl_2$ and $FeCl_3$ as starting materials to synthesis single doped TiO_2 and found out presence of Ferum ion influenced the photocatalytic activity instead of presence of Chloride ion which do not have any significance.

Besides the concentration of dopants, pH values also have significant effect toward the photocatalytic activity. pH solution influenced on azo Orange Dye (OG) was investigated by Sun et al. (2008) using nitrogen doped TiO_2. The result found that decreasing pH value from 6.5 to 2.0 had increased the degradation efficiency of OG from 31.67 to 98.98% in 150 min of visible light irradiation and from 8.00 to 99.37% in 60 min of natural sunlight. Platinum single doped with TiO_2 showed increasing of photocatalytic activity toward oxidation of Nitrogen Oxides ranging pH from 3 until 7. But later photocatalytic activity decreased when pH was further increased [48]. Zinc-doped TiO_2 was synthesis by Reynoso-Soto et al. [38] showed 10, 99 and 90% degradation efficiency of nitrobenzene (NB) ranging pH from 4, 7 and 10, respectively. The results revealed that under acidic condition, degradation of NB can occur effectively and negligible changes were observed under alkaline condition. This is due to the zeta potential of Zinc doped TiO_2 that acts as a strong Lewis due to surface positive charges.

Previous study also proved that doping will produce small crystallite

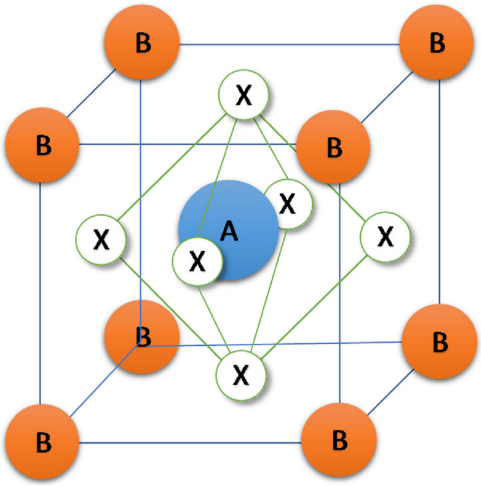

Fig. 1. Simple structure of perovskite ABO_3 crystal.

size thus enhancing the photocatalytic activity. Co-doped of Carbon-Yitrium with TiO_2 can prevent the size growth of catalyst [37]. Zinc-doped TiO_2 as synthesised by Reynoso-Soto et al. [38] also portrayed the same result. Increasing the content of dopants eventually decrease the size of crystal which is good for the degradation of Nitrobenzene [38]. The photocatalytic activity of Ferum-ion-doped TiO_2 as synthesised by Zhu et al. [45] showed that 0.09% Fe(II) ions-TiO_2 and 0.09% Fe(III) ions –TiO_2 exhibited best performance in degradation of XRG dye due its high surface areas and small crystal sizes.

2.2. Perovskite

Perovskite are generally classified to compounds possessing the formula of ABO_3 [49]. Perovskite crystal oxide structure consists of larger A cation with smaller B cation in an octahedral configuration (Fig. 1), where A is an alkali rare earth such as La, Ca, Sr, and Ba; and B is an element with valence +3 or +2, such as Fe, Cu and Ni which exhibits high proton and oxygen ion conductivity [50]. Perovskite oxides have been of great importance since the material exhibits a wide range of beneficial properties which include magnetic, superconducting and dielectric [21,51]. Recently, perovskite-based photocatalyst is another type of photocatalyst that had received tremendous attention due to its visible-light-driven properties. It consists of a few different types of photocatalyst which are titanate perovskite, tantalate perovskite, vanadium and niobium-based perovskite and ferrite perovskite. Some few example of perovskite type photocatalyst are shown in Table 2. One of the promising material as efficient visible-light driven photocatalyst in photocatalytic reactions is semiconductor lanthanum orthoferrite ($LaFeO_3$) due to its narrow band gap and optoelectronic properties [18]. Thirumalairajan et al. [50] had successfully synthesized perovskite $LaFeO_3$ microspheres using hydrothermal method [50]. They have found that the optical band gap of the synthesized $LaFeO_3$ is E_g = 2.06 eV using the formula, $E_g = 1240/\lambda_g$. This indicates that the $LaFeO_3$ had bright potential to be applied as a visible-light-driven photocatalyst. Moreover, from the Brunauer–Emmett–Teller (BET) characterizations, they found that the synthesized $LaFeO_3$ have sufficient specific surface area of 8.5 m^2/g, which can promote the degradation of organic dye in aqueous solution.

Table 2
Perovskite type photocatalyst.

Type	Formula	Band gap (eV)	Ref.
Titanate perovskite	$CoTiO_3$	2.28	[19]
Tantalate perovskite	$NaTaO_3$	4.2	[20]
Niobium perovskite	$KNbO_3$	3.14–3.24	[21]
	$NaNbO_3$	3.0–3.5	[22]
Vanadium perovskite	$PbVO_3$	2.93	[23]
	$SrVO_3$	3.22	[23]
Ferrite perovskite	$LaFeO_3$	2.1	[24.25.53]
	$YFeO_3$	2.43	[26]
Others	$NaBiO_3$	2.53	[27,28]
	$AgBiO_3$	2.5	[29]
	$LaNiO_3$	2.26–2.51	[30,31]
	$SrSnO_3$	4.1	[32]

Li and Feng [52] had synthesized visible-light responsive La_2O_3/TiO_2 nanotube arrays (TNTs) composite by a facile impregnation-calcinations technique [52]. The synthesized La_2O_3/TiO_2 was found to have the optical band gap of 2.99 eV with highest photocatalytic degradation efficiency (56%) compared to pure TNTs under visible light illumination. This is attributed by the high surface area and sufficient active sites to adsorb the RhB molecules on the surface of the photocatalyst. Perovskite praseodymium ferrite ($PrFeO_3$) porous nanotubes has been successfully prepared by Qin et al. [5] via electrospinning method [5]. They demonstrated that the porous tubes were attached with perovskite-type $PrFeO_3$ crystals with high optical absorption in the UV–vis region and an energy band gap of 1.97 eV. They have also compared the photocatalytic activity of $PrFeO_3$ nanotube, porous fiber and nanoparticles structure and found that 46.5% RhB is degraded by the nanotube sample in 6 h, while for the porous fiber and nanoparticle samples; the decolorization efficiency was only 29.5% and 15.7%, respectively. The main reason for this phenomenon is the highest specific surface area of the nanotubes itself.

Based on the aforementioned researches, it can be highlighted that perovskite photocatalyst highly dependent on its morphology and particle size. This is due to the heterogeneous process in photocatalysis that makes the surface area of applied semiconductor as one of the crucial parameters on efficiency of light absorption and pollutant adsorption. Previous researchers have found that some effective ways to increase the surface area of photocatalyst such as fine tuning the morphology of photocatalyst to smaller size or nanoparticles [50,54], and immobilization of the photocatalyst on the surface of an appropriate adsorbent [52,53,55–58].

2.3. Others

Graphitic carbon nitride (g-C_3N_4), a new-type polymeric semiconductor material with narrow bandgap, is widely used in photocatalytic degradation of organic and inorganic pollutants [59]. Somehow, g-C_3N_4 is still limited by its low visible light absorption, rapid recombination of photogenerated electron/hole pairs and low photocatalytic performance. Thus, numerous strategies have been applied to enhance the photocatalytic properties of pure g-C_3N_4 such as integrating g-C_3N_4 with metal oxides or other semiconductors to form heterojunctions [59,60]. Superior visible-light responsive photocatalytic activity for the degradation of rhodamine B has been observed by Sun et al. (2016) for Ag/g-C_3N_4 [60]. The enhancement in the intensities of the visible light has been observed with the addition of Ag in g-C_3N_4 due to surface plasmon resonance (SPR) of Ag nanoparticles. Besides, this photocatalyst also exhibit higher suppression of the electron-hole recombination process.

Bi_3O_4Cl is a semiconductor photocatalyst with narrow band-gap (2.76 eV) with uniquely layered structure, as shown in Fig. 2, which makes the semiconductor hold strong ability in the separation of photogenerated charge carriers [61–63]. Both properties makes it suitable for photocatalytic activity. Huang et al. [61] further improved the photocatalytic activity of Bi_3O_4Cl by synthesizing AgCl/Bi_3O_4Cl composite [61]. The BET results show that surface area of AgCl/Bi_3O_4Cl composite is higher than pristine materials. This reflects that AgCl/Bi_3O_4Cl composite had higher adsorption capacity which is beneficial for the photocatalytic activity. The stronger photoabsorption ability for visible light of the AgCl/Bi_3O_4Cl composite is due to surface plasmon resonance (SPR) effect of Ag nanoparticles (NPs).

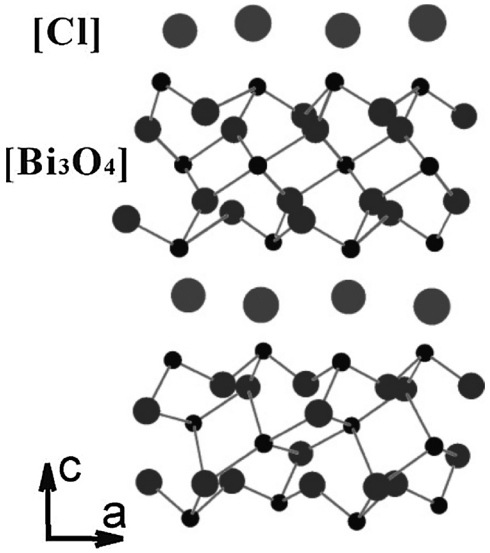

Fig. 2. The layered structure of Bi_3O_4Cl [63].

3. Adsorbents

Adsorbents have been used widely by many researchers for the removal of heavy metals and organic compounds in wastewater treatment [64–68]. There are varieties of adsorbents available such as activated carbon, zeolite, graphene oxide, silica oxide, zinc oxide, carbon nanotubes (CNT), CuO, polymeric adsorbents and many more [13,64,69–72]. Recently, researchers are also looking into less expensive materials as adsorbents such as agricultural and industrial wastes [73]. The examples of low cost agricultural by-products are sugarcane bagasse, rice husk, sawdust, coconut husk, oil palm shell, neem bark, orange peels [74] and others. Hegazi [73] used agricultural and industrial wastes such as rice husk and fly ash for the elimination of heavy metals from wastewater of electroplating industries in Egypt. They had found that rice husk was effective in the simultaneous removal of Fe, Pb and Ni, whereas fly ash was effective in the removal of Cd and Cu.

It should be noted that the performance of an adsorption process is affected by the adsorbent's characteristics and two adsorbents cannot be compared directly. Generally, there are few factors affecting the adsorption process such as surface area, intrinsic properties of adsorbate, concentration and dose of adsorbates, pH and temperatures. Table 3 listed some important properties of the adsorbents that have been previously used. Based on Table 3, it can be observed that oxidised carbon black (OCB) have the highest value of specific surface area, and study by [65] found that the adsorption capacities followed the order of OCB > CB > organic bentonite > bentonite, which was dependable with the orders of their specific surface area. However, study by [16] highlighted that besides having high specific surface area, an effective adsorbents should possess heterogeneity in pore size and shape and a large pore volume (~6–9 Å). This is based on their observation that zeolites were less effective than the carbonaceous adsorbents, due to the uniform size and shape of zeolite pore that will only adsorb contaminant with matching pore size and shape.

There are different types of adsorption mechanisms of contaminants including functional groups in the surface of adsorbents, charge of the adsorbent and active site of the adsorbent, as shown in Fig. 3. It is known that materials with large amounts of active groups such as hydroxyl or carboxyl groups can be used to adsorb contaminants with high removal efficiency. Thus, many adsorbents used by previous researchers consist of functional groups on the surface of adsorbents such as work by Zhu et al. [13]. They have reported the application of macronet hyper crosslinked polymeric adsorbents (MN 500 and MN 200) for pyridine removal from aqueous solutions and observed that MN 500 have higher adsorption rate due to the presence of "reactive" sulfonic acid group in the surface of MN 500 [13]. In 2007, Fletcher et al. had observed the adsorption of water vapor in activated carbon with oxygen functional groups [77]. Later in 2015, Yu et al. discovered about the adsorption mechanism of Cu^{2+} on different types of adsorbents such as carbon black (CB), oxidized carbon black (OCB), bentonite and organic bentonite [65]. For CB and bentonite, the mechanism for adsorption was dominated by surface adsorption and ion exchange adsorption. While for organic bentonite, the adsorption happens due to the complexing reactions of organic compounds in clay interlayer with heavy metal ions. Lastly, the adsorption of OCB occurs by the oxygen containing functional groups chelate with heavy metal ion.

Table 3
Characteristics of adsorbents.

Adsorbents	Specific surface area ($m^2.g^{-1}$)	Zeta potential (mV)	Ref.
Kaolin	156.91	−37.324	[14]
Synthetic talc	793.00	−53.560	[14]
Macronet polymeric adsorbents 200	414.00	–	[13]
Macronet polymeric adsorbent 500	9.54	–	[13]
Bentonite	931.33	−17.50	[65]
Carbon black	1114.23	−6.06	[65]
Oxidized carbon black	157.00	−17.18	[65]
Ti-Al-O	433.00	–	[15]
Ti-Si-O	181.00	–	[15]
Al_2O_3	168.00	–	[15]
Zeolite X	0.0844	–	[75]
Montmorillonite	61.00	–	[76]
Graphene oxide	497	–	[72]
SWCNT	537	–	[72]
MWCNT	179	–	[72]
Zeolite Mordenite	505	–	[16]
Zeolite Y	806	–	[16]

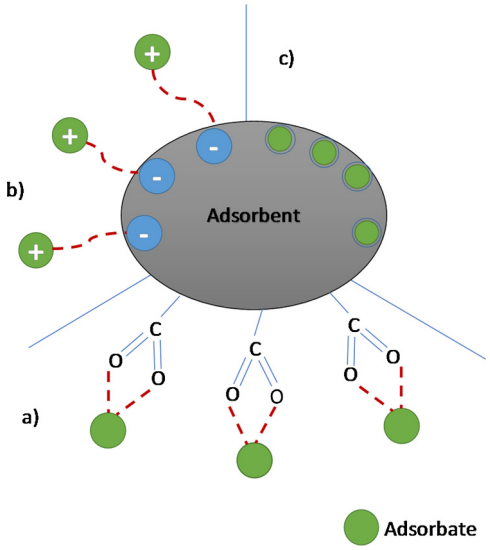

Fig. 3. Schematic diagram of the adsorption mechanisms of contaminants on adsorbents a) functional groups adsorptions, b) ion-exchange adsorption and c) adsorption capacity.

4. Integrated photocatalyst adsorbents (IPCA)

The integration of adsorption and photocatalysis processes could leads to several benefits to wastewater treatment. Such hybrid process

Table 4
Previous study on IPCA for organic contaminants degradation in waste water treatment.

	Catalyst	Adsorbents	Target compound	Degradation efficiency	Ref.
1	TiO_2	Zeolite	Amoxicillin	88 % (4 h irradiation time)	[82]
2	TiO_2	Zeolite	Dichlorvos	89.96%	[83]
3	Ag-CdZnSO	Zeolitic matrix	Disperse orange 30 dye	99.5% (90 min under UV light irradiation)	[84]
4	TiO_2	Zeolite	Acetophenone, phenol, and chloroacetic acid	–	[58]
5	TiO_2	Zeolite (ZSM-5)	Phenol	90% (180 min irradiation time)	[85]
6	Nano-TiO_2	Zeolite (ZSM-5)	Brown-NG (an azo-dye)	100% (20 min under UV irradiation)	[86]
7	Lanthanum loaded-TiO_2	Zeolite (ZSM-5)	Methyl orange	~97% (210 min under UV irradiation)	[87]
8	Yytrium incorporated TiO_2	Zeolite (ZSM-5)	Methyl orange	97.3%	[88]
9	TiO_2	5 A Zeolite	Oxytetracycline (OTC)	30.57% (10 h under UV light irradiation)	[89]
9	N- doped TiO_2	Diatomite	Tetracycline hydrochloride	90.2% (300 min irradiation time)	[90]
10	TiO_2 nanotube	Carbon-macroscopic monoliths	Methylene blue	100% (120 min)	[91]
11	ZnO	Clay	Methylene blue	100% (~180 min)	[92]
12	BiOBr	Graphene oxide (GO)	Rhodamine-B (RhB) and methylene blue (MB)	98% (RhB, 45 min) and 95% (MB,30 min) under visible light	[93]
13	TiO_2	Kaolin	Anions PO_4^{3-} and NO_3-	100% PO_4^{3-} and 65% NO_3-	[79]
14	ZnO	Graphene	Rhodamine B	100% (45 min irradiation time under UV light)	[94]
15	$CeVO_4$	Graphene	Methylene blue	98% (18 min irradiation time under visible light)	[28]
16	TiO_2	Activated carbon	Indomethacin	70%	[95]
16	Ag/AgBr	Activated carbon	Methyl orange (MO) and phenol	MO: 95.4% (2 h irradiation time under visible light) Phenol: 7.6 mg phenol per gram of composite in 3 h of irradiation	[96]
17	CuO/Cu_2O	β-cyclodextrin-modified carbon fibers	2, 6-dichlorophenol	87.5% (12 h irradiation time)	[10]
18	ZnO_2	Chitosan	Methyl orange (MO)	80% (100 min irradiation time under UV light)	[97]
19	TiO2	CNT	Methyl orange (MO)	100% (100 min irradiation time under UV light)	[98]
20	Ag-ZnO	Graphene	Methylene blue (MB), rhodamine B and methyl orange (MO)	97.8% (7 h irradiation under sunlight)	[99]
21	TiO_2	Activated alumina (AA)	Inorganic arsenic and organoarsenic compounds	98% (15 h under sunlight irradiation)	[100]
22	Fe_3O_4	Modified activated carbon	Methylene blue	100% (75 min under UV light irradiation)	[78]
23	C_3N_4	SiO_2	Methylene blue	90% (4 h under visible light irradiation in dynamic systems)	[101]
24	$CoFe_2O_4$	Activated carbon	Cr(VI)	Separation was efficient with magnetically separable Cr(VI)	[71]
25	Ag-CdZnSO	Zeolitic matrix	Disperse orange 30 dye	99.5% (90 min under UV light irradiation)	[84]
26	Ag-AgBr	MMT	Methylene blue	92% (20 min under visible light irradiation)	[102]

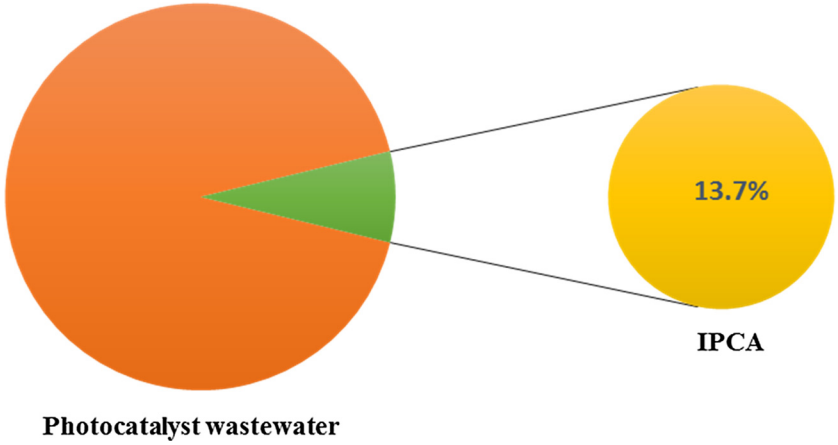

Fig. 4. Number of publications concerning integrated photocatalyst adsorbent for wastewater treatment. Search done through Scopus website in April 2018.

does not only preserve all the interesting characteristics of its individual components, but also overcomes serious drawbacks of each technique when operated individually, thus improving the overall removal efficiency. A lot of study has been conducted in employing IPCA for organic contaminants degradation in wastewater treatment as listed in Table 4. Most of the study reported on the improvement of degradation efficiency due to the increment in contaminants adsorption on photocatalyst surface by the adsorbents. Somehow, it is surprising that the numbers of publications concerning IPCA are very limited (see Fig. 4), approximately 13.7% from total publications in photocatalyst for wastewater treatment from 1989 to 2018. This reflects that more efforts are needed to establish this technology for wastewater treatment applications.

There are different methods that has been applied in integrating the photocatalyst with adsorbents such as microwave-assisted method [78], sol-gel methods [79,80], solution process methods, wet chemical impregnation [81] and more. A detailed survey of literature reveals no information on comprehensive study regarding the methods in integrating the photocatalyst with adsorbents. In fact, we believed that the interaction between photocatalyst and adsorbents have significant

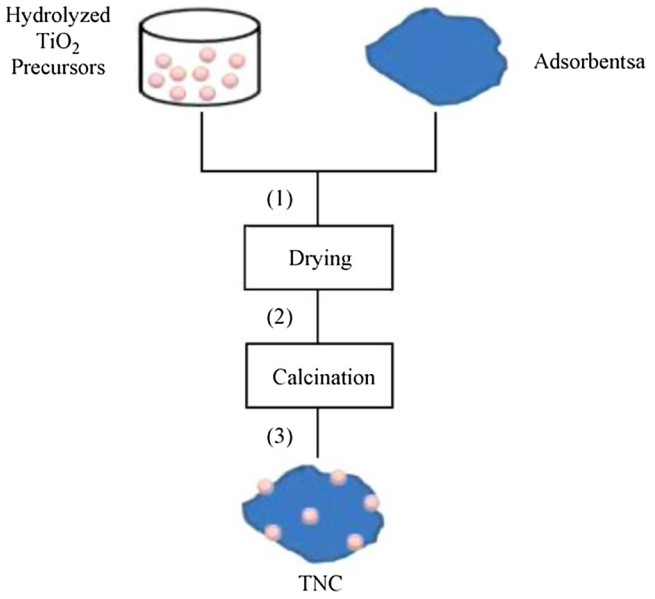

Fig. 5. A schematic wet chemical assembly of TNC [81].

effects in the adsorption and degradation performance of IPCA. In 2009, Zhang et al. has summarized the key variables in the preparation conditions and corresponding as-synthesized TiO_2/adsorbent nanocomposites (TNC) via wet chemical impregnation methods [81]. They had highlighted few parameters that may influence the properties of the synthesized TNC such as porous adsorbents, TiO_2 precursors, TiO_2 loading and location, solvent and pH value, and post treatments. Fig. 5 shows the typical process of wet chemical impregnation assembly of TNC.

Previous study had proposed a reaction mechanism between IPCA and targeted compound [53]. Fig. 6 showed the proposed photocatalytic degradation reaction mechanism which occurs in sequence. (1) The mechanism is initiated by the irradiation of visible light on photocatalyst which allow the movement of electron form valance to conduction band. (2) At this phase, GO as absorbent will deter the recombination of the separated electron while keeping them reactive on its surface. (3) Hydroxyl radicals was produced from the oxidation of hydroxide ion in water by photoinduced holes. (4) The electron continues to move across GO surface until it reacts with the dissolved oxygen. (5) Superoxide radical anions is produced by the reaction between migrating electron and dissolved oxygen. (6) Formation of hydroxyl radical is produced from the superoxide radical anions. Decomposition of targeted compound is initiated by the reaction of hydroxyl radicals to form non-toxic compounds. The absorbent would assist in concentrating the absorbent near the vicinity of photocatalyst to improve degradation.

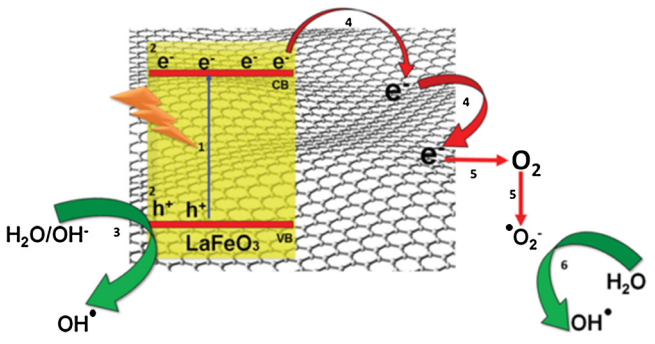

Fig. 6. Proposed mechanism of photocatalytic degradation of pollutant by IPCA [53].

Chong et al. [80] prepared the titania impregnated kaolinite (TiO_2/K) photocatalyst using two-step sol–gel method [80]. The optimum TiO_2/K loading was found at 6 g/dm^3 which is equivalent to 0.48 g/dm^3 of TiO_2. This result suggested that TiO_2/K with the annular photocatalytic reactor systems (APR system) have better photo-efficiency, as it requires lower TiO_2/K loading compare to pure TiO_2 mainly due to better adsorption capability of K which increases the probability of surface reaction with contaminants. Later in 2010, Vimonses et al. [79] compared the performance of TiO_2/K photocatalyst using two different systems namely APR and fluidised bed reactor (FBR). From their observation, the adsorption of pollutants through the FBR system has higher efficiency in removing the inorganic nutrients, especially for PO_4^{3-}, compared to APR systems. This finding reflects that different systems applied will have different performances, thus comprehensive study is needed in finding suitable systems for IPCA in suspended solids.

4.1. Criteria for selecting the adsorbents in integrated photocatalyst adsorbents (IPCA) systems

In selecting the adsorbents materials as support for photocatalyst-adsorbents composite, few criteria should be considered (see Fig. 7). Firstly, the adsorbents should be acting as support material which inhibits leaching of the metal oxides particles into the treated water. Leaching should be expected from integrated photocatalyst adsorbents materials because most of the composite incorporation involves only physical bonding [103]. Leaching phenomenon will demonstrate whether the adsorbents and photocatalyst in the composite has a good attraction or not. The selection of compatible adsorbents and photocatalyst is essential to allow the synthesized composite to possess good stability with dispersing solvent and reusability. The reusability factor of IPCA would be a huge advantage for industrial application. Somehow, most of the study on IPCA is neglecting this phenomenon completely. Nevertheless, limited publications could be found reporting on leaching of photocatalyst in IPCA systems. Colmenares et al. [104] demonstrated that Starbon in the composites has very good contact with the TiO_2 nanoparticles since there is no Ti leaching was observed in the XRF analysis [104]. It is believed that the ultrasound-induced impregnation method have promoted the TiO_2 anchoring on ordered mesoporous carbon thus enhanced its photocatalytic activity. Good compatibility between adsorbents and photocatalyst is necessary to ensure high reusability and stability of the nanocomposite. Adsorbents with active oxygen functional groups will also produce stables photocatalyst-adsorbents composites.

Secondly, the porous adsorbents must have high adsorption capacity for the target compound and yet the affinity should be moderate for the efficient diffusion of adsorbed substrates to the photocatalytic active sites. The affinity of the targeted contaminants toward the surface of adsorbent could be related to the ionic strength [105]. Anirudhan et al. [105] observed that the adsorption capacity of PAA-g-CGR/TNT composite decreases with an increase in the ionic strength [105]. This is mainly due to the formation of outer-sphere complexes of the composites with ions. It is also stated that ions that form inner-sphere complexes shows increase in adsorption with increase in ionic strength. Another study conducted by Liu et al. [106] employed Porous Boron Nitrate (BN/TiO_2) as a support host for photocatalyst, TiO2. Hybridation between these two materials were prepared via solvothermal process and create actively chemical bond, B-O-Ti [106]. The strong interaction bond resulted 99% degradation of photocatlytic activity within 6 h toward RhB dyes. The presence of TiO2 anchored on surface of porous BN simultaneously enhance the adsorption capability and lead the targeted pollutants on the surface through π-π interactions, thus increase the photocatalytic activity.

Thirdly, it should have a reasonable transparency to UV–vis light to allow the penetration of lights to photocatalyst. For example, graphene-based materials are a promising adsorbents candidate for IPCA systems. This is due to its intrinsic properties such as excellent transparency,

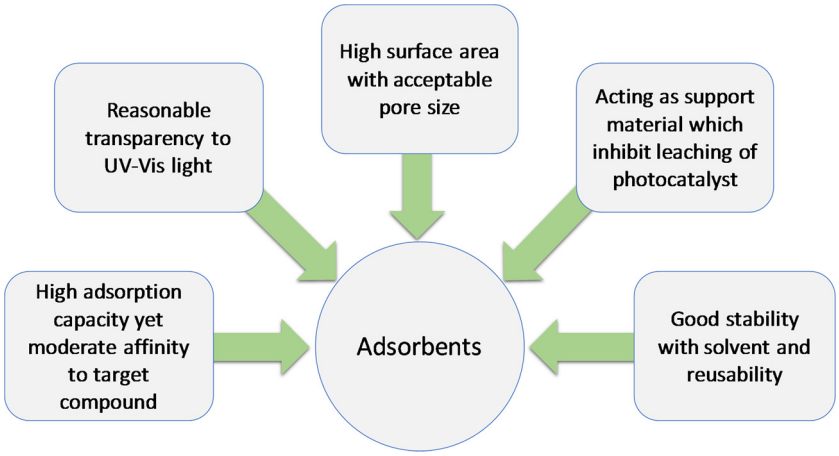

Fig. 7. Criteria for selecting the adsorbents in integrated photocatalyst adsorbents (IPCA) systems.

high specific area, superior electron mobility and high chemical and electrochemical stability [107]. Coarse-granular wide-pore silica has been applied by et al. [108] as an active adsorbent to coat a porous silica substrate with TiO_2-based nanoparticles for gas cleaning in a fixed bed reactor [108]. The resulting materials possess high adsorption capacity and high photocatalytic activity under UV-A illumination mainly due to high-specific surface area and acceptable UV-light transmission of coarse-granular wide-pore silica.

Lastly, the adsorbents should have high surface area with acceptable pore size. It is known that high surface area will promote high adsorption capacity thus increase the photocatalytic activity [109–113]. Taufik et al. [111] incorporated ternary mixed oxides on graphene and observed an increment in surface area of the nanocomposites [111]. It was found that graphene increased the surface area of the nanocomposites which consequently enhances the adsorption ability and photocatalytic activity of the nanocomposite. Study conducted by Shao et al. [110] demonstrated this phenomenon. They modified the surface area and pore size of MCM-41 by loading it with different loading of Mn as shown in Table 5. The adsorption study revealed that 1%Mn/MCM-41 had the highest adsorption capacity (45.38 mg/g) compared to other samples. This result clearly showed that surface area was not the only criteria in selecting the adsorbents for any applications.

Porosity of support adsorbent also gives an impact to the performance of degradation. Common types of porosity that are usually classified are micropores and mesopores. According to IUPAC, range for micropores is less 2 nm and for mesopores is between 2 and 50 nm. Typically, adsorbent that related to micropores type is zeolite and activated carbon. Excessive concentration of photocatalyst could inhibit the adsorption capability and lower the photodegradation activity but somehow can prevent from this happening if the pores of material is small. Immobilization of TiO2 on commercial activated carbon, (QTi) has been extensively studied by Velasco et al. [114]. The photocatalytic activity was observed on composite of QTi under UV light irradiation and showed 98% degradation of phenol. This could be explained based on N_2 adsorption data, titania was unable to enter into inner microporosity of the carbon and the pores of carbon remain unblocked. Other significant reasons is by the weak interactions occurring between the carbon surface and titania (supported by the slight change in the pH_{PZC} in the composite) was possible in altering the mechanism of phenol photodegradation [114].

Although microporous provided high ability for efficient adsorption, some of the molecules cannot penetrate into limited sizes of pores. Typically, material that is related to mesoporous material is silica. The development study regarding mesoporous material are extensively rapid which mostly aim to produce larger pore catalysts, increase high diffusion rates and toward improvement of photocatalytic activity for larger molecules [115]. Adsorption capability of mesoporous material toward Cu(II) removal efficiencies has been conducted by Wu et al. [116]. In that study, the material were prepared by fly ash via hydrothermal method and discovered when increasing the Si:Al ratio, the adsorption capacity was able to reach maximum value as calculated (221 mg g^{-1}). Other study performed by Busuioc et al. [117] dispersed the composition of anatase titania on inert support material, mesoporous silica (SBA-15) [117]. Low loading concentration of titania (SBA–TiO_2-0.6) resulted high adsorption capacity of 88.3% but lowers the photocatalytic activity (14.3%). In contrast, when the loading of titania ((SBA–TiO_2-2) was increased, the adsorption capacity dropped to 44.5% but improved in photocatalytic activity (27.8%). The possible reason concluded from the results is when low amount of Titania is applied on the SBA support material, anatase titania crystal is still at early stage and thus diffusion into the pores is high and adsorption mechanism is favoured. Meanwhile, when the loading of titania was increased on SBA support material, formation of larger anatasa titania caused slow diffusion into pores of SBA support material and would favour toward self-photoactivity.

Table 5
Pore diameter, pore volume and surface area of MCM-41 and 0.5–4% Mn/MCM-41 [110].

Sample	S_{BET} ($m^2 g^{-1}$)	Pore diameter (nm)	Pore volume ($cm^3 g^{-1}$)
MCM-41	1025	2.71	1.28
0.5%Mn/MCM-41	938	2.68	1.14
1%Mn/MCM-41	921	2.53	1.06
2%Mn/MCM-41	854	2.1	0.89
4%Mn/MCM-41	838	2	0.76

4.2. Photocatalyst- activated carbon IPCA

Activated carbon (AC) is sourced from the combustion of carbonaceous material such as coal or plant-based [12,118]. The fabrication of AC would usually consist of carbonation and activation stages. The application of AC as the support and absorbent for photocatalyst has been applied by many researchers for many type of composites including Doped TiO_2/AC [119], Ag/AgCl/AC [120–122], ZnO/AC [123], Ce/AC [124] and others, as listed in Table 6. Principally, the presence of AC would allow more pollutant to be in contact with the photocatalyst to increase the degradation rate through absorption mechanism.

The presence of organic pollutants has been a major concern by researchers nowadays. Photocatalysis is viewed as one of the most promising technology to degrade organic pollutants in wastewater,

Table 6
Different type of works combining photocatalyst with AC for photocatalysis applications.

Photocatalyst	Fabrication method	Absorbent coating method	Irradiance	Model pollutant	Ref.
N-doped TiO_2	Vapour hydrolysis	Impregnation	Visible light	N/A	[119]
Ag/AgCl	photoreduction	Impregnation	Visible light	tetracycline	[120]
Ag/AgCl	photoreduction	Impregnation	Visible light	Escherichia coli K-12	[122]
Zn^{2+} doped TiO_2	Sol gel	Impregnation	UV	Tuolene	[125]
F-doped TiO_2	Sol gel	Rotary evaporator	Visible light	Phenol	[126]
WO_3-TiO_2	Sol gel	Impregnation	UV	azo dye Congo Red	[127]
ZnO	N/A	Rotary evaporator	UV	alizarin cyanin green dye	[123]
Ag-TiO_2	MOCVD	MOCVD	UV	Methyl orange	[128]
Fe_3O_4-TiO_2	Sol gel	Rotary Evaporator	UV	phenol	[129]
Ce	Sol gel	Impregnation	UV	4-chlorophenol	[124]
Fe(III)/Ho(III) co-doped TiO_2	Sol gel	Impregnation	UV	Methyl orange	[130]
PEI-AC	Hydrothermal				

with TiO_2 as the photocatalyst which non-toxic, chemically stable, economically feasible and activation by UV irradiance [131]. Also, TiO_2 doping is also studies rigorously to modify the characteristic of TiO_2 towards visible light reactivity. It was proved that the synergistic effect of AC with TiO_2 would improve the photodegradation rate [132]. Doped TiO_2 that have been documented includes N-doped [133], Zn^{2+}-TiO_2 [125], F-doped [126], WO_3-doped [127], Ag-doped [128] and others.

Huang et al. [119] have combined the impregnation and vapour-hydrolysis to develop nitrogen doped TiO_2 coated on AC [119]. The visible light activated photocatalyst was produced in anatase form with grain size of 10–20 nm. It was noted that, although TiO_2 dispersion onto activated carbon could enhance the photocatalytic activity, the active surface for activated carbon could be jeopardized by the hindering TiO_2 [134]. Nevertheless, the study has demonstrated high specific surface area of 1321 m^2/g by using the combined technique.

Zn^{2+}-TiO_2/AC composite was successfully fabricated using sol-gel method for the degradation of toluene under UV irradiation [125]. It was mentioned that the photocatalytic activity was enhanced due to the doping of Zn^{2+} compared to bare TiO_2/AC photocatalyst. Nevertheless, it was observed that 20% Zn doping was the best loading as higher content of large bend-gap energy of Zn would block the light absorption of TiO_2. Additionally, the obtained photocatalyst have sustained higher degree of photocatalytic degradation efficiency compared to bare TiO_2.

By using sol gel method, F-doped TiO_2/AC was successfully fabricated for the degradation of phenol under visible light irradiation [126]. It was mentioned that the F doping have inhibited grain growth, improve crystallinity and improve photocatalytic activity in visible light region. As expected, incorporating AC was also able to improve to more than 3 times specific surface area and at least doubles the pore volume compared to bare F-doped titania.

WO_3-TiO_2/AC photocatalyst was successfully fabricated for the degradation of azo dye Congo Red under UV irradiation [127]. Interestingly, it was demonstrated that the highest degradation performance was recorded with 10 g/L catalyst, pH 7 and 114 mM of H_2O_2. Also, the presence of ClO^{2-}, BrO^{3-} and $S_2O_8{}^{2-}$ would increase the photo-decolorization, while $SO_4{}^{2-}$, NO^{3-}, Cl^-, $SO_3{}^{2-}$, $H_2PO_4{}^-$ would decrease photoreduction activity. In addition, it was demonstrated that the photodegradation of azo dye Congo Red were found to follow pseudo-first-order reaction kinetics.

Plasmonic photocatalysis Ag/AgCl/AC was successful develop by using sodium citric as the complexing agent [120]. The method applied was demonstrated to be able to manage the size of AgCl by controlling the release of Ag ions by the formation of complex structure. The photodegradation reaction was initiated upon visible irradiation of Ag to produce electron-hole pairs [121]. The AgCl/Ag synergistic effect will retard the recombination rate and the positively charge holes subsequently travelled to AgCl for the oxidation of Cl ions to the atomic state. The atomic Cl is very reactive with high oxidation activity, will subsequently react with the pollutant and finally reduced to Cl ions again. The photogenerated electron would also be able to degrade organic pollutants by forming hydroxy radical with dissolve oxygen [135]. AC in this composite would promote pollutant adsorption for increased active reaction sites and ultimately increasing the degradation rate.

Ag/AgCl/AC composite can also be applied to inactivate bacteria (possess microbial property). A study has fabricated Ag/AgCl/AC composite to inactivate *Escherichia coli* K-12 in visible light irradiation [122]. The study has mentioned although the incorporation of biocidal silver atom would, to some extent, contribute to the inactivation of bacteria, the photo-induced reaction species were found to be possess more bacterial inactivation rate. Additionally, bacteria death is associated with the radical attack towards the cell wall, as observed on the changes of the cell structure and permeability.

ZnO photocatalyst supported on porous activated carbon was successfully assembled using rotary evaporator for the degradation of alizarin cyanin green dye in UV light [123]. As expected, ZnO/AC composite has higher photodegradation rate compared to bare ZnO due to the synergestic effect between ZnO and AC. Also, it was demonstrated that higher pH values would retard the photodegradation rate, while lower pH would promote the mineralization of the pollutant.

By using metal organic chemical vapor deposition (MOCVD) method, Ag-TiO_2 assembled on AC was successfully fabricated for the degradation of methyl orange under UV light [128]. The MOCVD method was advantageous over traditional method which would involve saturation, aging, drying, and reduction, that will inherently effect the performance of the catalyst. Additionally, this method promotes excellent photocatalyst cluster distribution on porous media which is beneficial for high catalytic efficiency.

Anatase titania-coated magnetic activated carbon (TMAC) was fabricated using sol gel method for the degradation of phenol under UV irradiation [129]. The photocatalyst was assisted by magnetic core (Fe_2O_3) and absorbent (AC), in order to introduce magnetic seperability and increase the adsorption activity, respectively. As expected, the photocatalytic activity of TMAC under UV light was higher when compared to titania coated AC, commercial titania and bare TiO_2 synthesised under the same method. Additionally, it was mention that the photocatalyst can be separated from the slurry solution by introducing external magnetic field and be redeployed into an aqueous solution by using ultrasonic vibration. Nevertheless, the study did not present the recyclability data to support this claim.

Ce/AC composites was successfully fabricated by using impregnation method for the degradation of 4-chlorophenol [124]. The study fabricated the Ce catalyst from its nitrate salt form by using sol gel method and impregnates the AC during the fabrication. As expected, the Ce/AC was found to possess higher degradation rate compared to bare Ce. Additionally, it was mentioned that the degradation reaction mechanism by using Ce as photocatalyst yield the same intermediates (hydroquinone and benzoquinone) as titania photocatalyst.

Apart from degradation of pollutant, chromium (Cr(IV)) adsorption

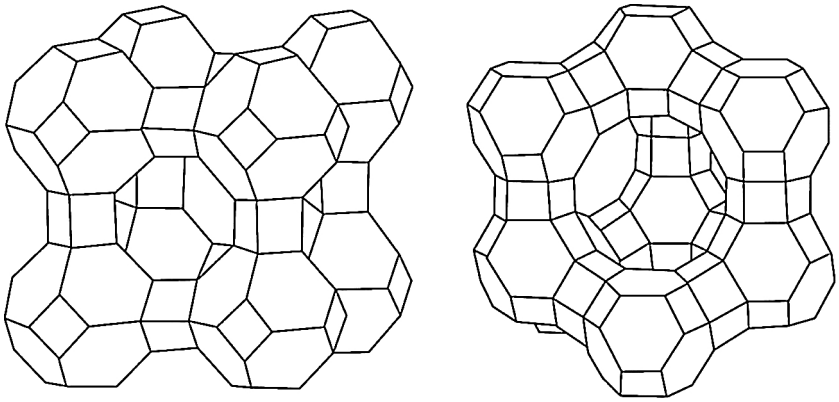

Fig. 8. a) Zeolite A and b) faujasite-type zeolites X and Y [144].

application have also added AC as in additive ingredients. $CoFe_2O_4$/AC was successfully fabricated by using hydrothermal method to effectively separate chromium from aqueous solution [136]. The results indicated that the adsorption of chromium was enhanced with the modification of spinel $CoFe_2O_4$ on AC surfaces. Although the specific surface area was reduced at the introduction of CoFe2O4, the adsorptive activity of $CoFe_2O_4$ towards Cr was higher. Additionally, magnetic separability was introduced to the AC due to the magnetic properties of spinel $CoFe_2O_4$.

AC support absorbent would usually present in powder form. Nevertheless, AC can also function as a support absorbent in fiber form [137]. Activated carbon fibers (ACF) has been applied as a support absorbent for Fe(III) and Ho(III) co-doped TiO_2 for the degradation of methylene orange in UV irradiation [130]. It was observed that the surface morphology of the ACL is dependent on the calcination temperature applied. Additionally, the co-doping of metals was able to supress the formation of cracking on ACL when subjected to high calcination temperature.

4.3. Photocatalyst – clays IPCA

Approach using clay minerals and clay-derived materials as adsorbents have high potential to be applied soon due to its abundance amount on the earth and low-cost materials. Clays can be classified into four groups which consist of kaolinite, montmorillonite– smectite, illite and chlorite. They portray porous heterostructures that turned them from inert form function to substantial roles in adsorption. Clay also have been identified as a good adsorbent due to its wide surface area, stability factor in term of chemical and physical, phyllosilicates material and high cation exchange capacity [138,139].

With a great structure and several specialities owned by clay, such as its wide application as adsorbents integrate with other photocatalyst, clays had received numerous attention in wastewater treatment applications. Previous study illustrated effect of ZnO contents in Nano-ZnO/Bentonite [140]. Result from this study showed that the photocatalytic activity was increased with ZnO content ranging from 10% to 60% while decreased when ZnO content went up to 70%. Excessive amount of ZnO had prevented Bentonite to function well as ZnO had dominated the hybrid. Higher degradation rate of Orange G done by previous study was observed when employed TiO_2 supported on Palygorskite clay mineral [141]. The study revealed that optimum concentration of TiO_2 supported Palygorskite clay which is only 0.4 $g{\cdot}L^{-1}$ lower than concentration of pristine TiO_2 [142]. Below the optimum concentration, complete radiation toward surface of particle was achieved due to excess of photon correspond to high surface area that exhibited by TiO_2 – Palygorskite [141].

One of the common effects that have been observed when integrating the photocatalyst into clays is the band gap increment of the composite compared to pristine photocatalyst [25,102,143]. Peng et al. [25] employed $LaFeO_3$/montmorillonite for degradation of Rhodamine B (RhB) under visible light irradiation [25]. This IPCA portrayed increment in band gap value of 2.24 eV higher than pristine $LaFeO_3$ which only 2.15 eV. They suggested that the larger band gap is attributed by the lower size of $LaFeO_3$ nanoparticles accumulated on montmorillonite surface. Despite of these values, $LaFeO_3$/montmorillonite still possessed good adsorption efficiency and had excellent photocatalytic activity due to better deposition of $LaFeO_3$ nanoparticles on montmorillonite surface, thanks to Si-O-Fe bonds [25]. Belver et al. [143] also observed a reduction in band gap after immobilizing Zr-doped TiO_2 nanoparticles on delaminated clay materials [143]. This is due to slight deformation of the anatase crystal by Zr-dopant. Somehow, high degradation rates could be observed due to homogenous distribution of anatase nanoparticles of Zr-doped TiO_2 over delaminated clay layers that increases the photocatalyst surface area. Sohrabnezhad et al. [102], also observed increment in band gap for Ag/AgBr–MMT nanocomposite compared to bulk Ag/AgBr [102]. The larger band gap is attributed to the multiple plasmonic oscillation frequencies present due to the variation in the shapes and diameters of Ag nanoparticles formed. Higher photoactivity was observed in Ag/AgBr–MMT nanocomposite compared to Ag/AgBr. This is because the MMT in Ag/AgBr–MMT nanocomposite not only acts as the adsorbents, but also minimized the electron–hole recombination in nanocomposite.

4.4. Photocatalyst – zeolite IPCA

Zeolites are hydrated alumino silicate minerals containing aluminium, silicon, and oxygen in their regular framework. Compositionally, zeolites are similar to clay minerals; however, they are differing in their crystalline structure. Fig. 8 shows the structure of zeolite A and faujasite-type zeolites X and Y formed by sodalite cages. Zeolite is considered important adsorbents due to its high extensive surface area, charged framework with amphoteric properties and high adsorption capacity [87]. Besides, its unique Al–O units in zeolite framework that able to reduce the electron electron–hole recombination process, making it as a promising candidates for hybrid adsorbents-photocatalyst applications [85].

Zainudin et al. [85] had proposed the mechanism of the photocatalytic activity of ZSM-5-TiO_2 IPCA [85]. The ZSM-5 acts as the adsorbents that concentrate the pollutants to the photocatalytic surface which consequently increases the photocatalytic activity of the photocatalyst. The same phenomenon was observed by previous studies ([84,89,82]) for the degradation of dyes and amoxicillin over Ag-CdZnSO/zeolitic and TiO_2/zeolite matrix nanocomposites, respectively. Jaime-Acuña et al. [84] had highlighted the adsorptive capacity of the

zeolitic matrices, which permits closer contact between the organic molecules and the supported nanoparticles by a local concentration effect, is one of the contribution to higher degradation of dyes. Meanwhile, Kanakaraju et al. [82] believed that the acidic nature of the TiO_2/zeolite may have assisted degradation of amoxicillin by partial hydrolysis [82]. Zhao et al. have different ideas about the adsorption mechanisms of contaminants on adsorbents [89]. They proposed that electrostatic attractions are the mechanism for the adsorption of organic molecules on adsorbents and based on their study, at high pH (pH $\geq$ 11), electrostatic repulsion minimized adsorption.

Due to variety of special properties exhibited by zeolites, the adsorbents help in improving photocatalytic activity. Guesh et al. [145] demonstrated photodegradation on methyl orange (MO) and real textile wastewater of Ethiopia using zeolite hybrid TiO_2. 10% concentration of TiO_2-Zeolite Y (CBV 760) showed 20 times higher mass normalized turnover rate (TORm) and also resulted in 84% elimination of total organic carbon (TOC). Performance of photocatalytic activity by using hybrid TiO_2-zeolite reported in the study is higher than using pure TiO_2 only. This indicated hybrid TiO_2-zeolite have speciality in lower of recombination electron/holes pair. [145].

Other than, presence of zeolite as adsorbent in photocatalyst helps in improving photodegradation of pollutant due to its hydrophobic nature. Takeuchi et al. [146], prepared high silica mordenite (MOR) zeolite blended with TiO_2 in agate mortar [146]. The study revealed that high hydrophobic properties of zeolites leading to increase in photocatalytic oxidation of gaseous acetaldehyde [146]. Takashi et al (2013) performed photodegradation towards 2-propanol by using Y-zeolite with variable of SiO_2/Al_2O_3 ratio and two different kinds of TiO_2 precursors, i.e., titanium ammonium oxalate and ammonium hexafluorotitanate [147]. Photocatalytic activity also is enhanced by hydrophobic nature of zeolite due to high polarity of 2-propanol. Thus, it can be concluded that designing the IPCA for specific target contaminants can be done by choosing an appropriate adsorbent with particular properties.

4.5. Photocatalyst – graphene

Graphene is founded initially in October 2004 by two physicists known as Geim and Novoselov and won Nobel Price later in 2010 for prioritizing Graphene in their work. Since that, graphene and its derivatives has been widely studied which including Graphene Oxide (GO) and Reduced Graphene Oxide (RGO). The structure of Graphene (GR) is made up of single layer of sp2 bonded and becomes basic unit of carbon, CNTs and fullerenes [148]. GR is denoted as impressive material as it portrayed special characteristics. This material is good in conductivity, has high chemical stability [149,150], high mechanical strength and even high surface area (2630 $m^2 g^{-1}$) [151]. Soon the researchers realize the beneficial aspects showed by GR for the applications of photocatalysis.

One of the crucial issues in photocatalysis is the recombination of electron-holes pair that reduces the photocatalytic activity. The presence of GR as an adsorbent carbon combine with semiconductor photocatalyst can be functioned well as an efficient carrier for electron and holes. The capability of GR that able to prevent electron-hole recombination has been studied by Wang et al. (2010). They demonstrated photoinduced data between TiO2 and GR via a transient photovoltage method and found that the meantime were increased from 10-7 s to 10-5 s when TiO_2 combined with GR [152]. Lightcap et al. [153] confirmed the role of GR in electron transfer by determining the color of solution as shown in Fig. 9 [153]. Later in 2011, they conducted an experiment on the GO suspension with ZnO to observe the electron transfer ability of GO. The GO suspension with ZnO were irradiated with UV light and it has been observed that the mean lifetime of ZnO emission were decreased from 30-14 ns when increased GO loading [154].

Recent literatures have outlined that the GR supported on photocatalyst produced notable photocatalytic performance mainly due to the enhancement in adsorption rate of pollutant and light absorptivity of the composite [155,156]. Additionally, GR also can act as sensitizer to improve the efficiency of IPCA toward light irradiation and lead to high efficiency of photocatalytic activity. One of GR derivatives, GO possess good quality material for supported photocatalyst since it contains a range of reactive oxygen functional groups such as carbonyl, epoxy and hydroxyl groups on the surface. This makes GO able to have interaction with a wide variety of molecules and thus can undergo surface modification [4].

One of the main factors that have been proved to have significant effects toward enhancing photocatalytic activity is catalyst loading. Catalyst loading effect is known can increase the photocatalytic activity and thus, increase the efficiency of degradation toward pollutants. Nevertheless, increasing loading of catalyst until it approach certain threshold limit could inflict a reduction in photocatalytic activity through enhancing absorption and scattering of photons by excess carbon content present in the composite [157]. For that cause, graphene loading contents behave importantly in deciding photocatalytic activity of the composite.

Earlier work in varying Graphene loadings has been conducted by Wang et al. (2012). They observed that 0.05 wt% of graphene integrated with TiO_2 produced the highest performance in photocatalytic degradation of contaminants [158]. Alim et al. [159] studied the performance of reduced graphene oxide with anatase TiO_2 by varying the loading and discovered optimum loading of reduced graphene oxide with (3 wt%) exhibited more than 4 times photocatalytic activity compare to bare anatase TiO_2 [159]. It was proved from the study, the presence of reduced graphene oxide onto anatase TiO_2 suppressed the recombination of electron-holes pair. Another photodegradation performed by Zubir, (2015) on synthetic dye acid orange 7 (AO7) employed GO–Fe_3O (Graphene Oxide-Iron Oxide) composites. The result shows that the degradation rate was high (92–98%) at low GO loadings $\leq$10 wt% that may be due to the high surface area (409 $m^2 g^{-1}$) of the composite [160]. The performance of degradation dropped at GO loading > 10 wt% (60%) and at the same time the surface area is reduced. The achievement performance by GO–Fe_3O can be explained by presence of strong interfacial interactions (Fe–O–C bonds) that occur in the nanocomposites.

4.6. Others

Chitosan is polysaccharides adsorbent that start to seek attention from researchers recently. Chitosan is synthesis by alkaline deacetylation of chitin. Chitin can be found abundantly at coastal area. One of abnormality described by chitosan is its polysaccharides behave as alkaline nature while most of polysaccharides behave in acidic nature. Chitosan can see as a potential absorbents applied in wastewater treatment in future as it is renewable, nontoxic, biocompatible and degradable [161]. Besides that, its speciality which can exhibits high affinity to adsorb pollutants such as heavy metal [162] and dyes [163], which can attract industry attention to develop chitosan as an absorbents in wastewater treatment. Chitosan portrays good adsorption towards pollutants such as heavy metal is because its amine and hydroxyl groups behave as active sites for heavy metal and anionic organic pollutants [164].

The ability of chitosan as a potential adsorbent creates an idea for the researchers to bind with photocatalyst especially for degradation of emerging contaminants. Chitosan hybrid with zinc oxide (ZnO) has achieved 85% removal of ethyl orange at 60 °C. The study reported increasing dosage of zinc oxide enhanced the removal of dyes [165]. Haldorai et al. [166] prepared chitosan hybrid with copper oxide (CuO) for the degradation of Methylene Blue (MB). The photodegradation under UV irradiation resulted 84% removal of MB [166]. Other fascinating study illustrated by Zainel et al. [167] bind Chitosan with TiO_2 coated onto glass plates and resulted 87% removal of Methyl orange

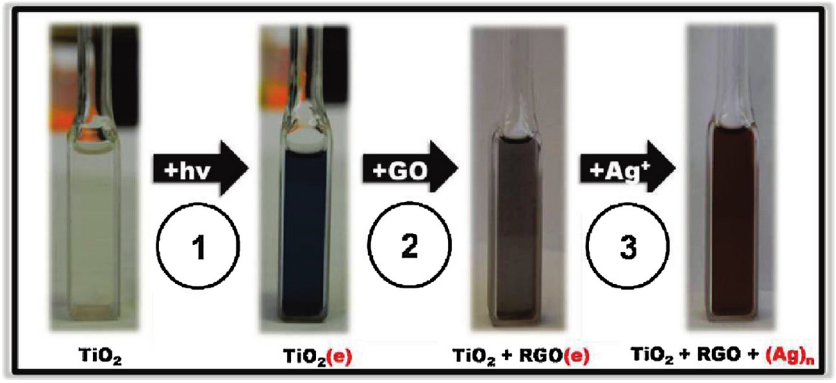

Fig. 9. The images showing a sequence of changing color during stepwise transfer of electrons (1) Storing electrons in TiO2 by irradiating the sample with UV light (λ > 300 nm) for 30 min. (2) Addition of GO until no blue color remains. Gray-colored solution is forming due to the formation of RGO. (3) Reduction of Ag + to Ag nanoparticles (red color) by stored electrons in RGO following the addition of $AgNO_3$ solution.

(MO) [167].

Other than chitosan, silica also has been identified to have potential as a good absorbent. Silica has portrayed its ability in adsorption process, catalyst support, drug absorbents and others. Variety application in worldwide covered by silica is because of its several substantial properties such as high porosity, wide inner surface area, and also high adsorption properties of the available materials. As the silica has been viewed as a promising absorbent, many study demonstrated silica with photocatalyst to discover the effectiveness of each material. Wang et al. [168] have prepared silica gel supported-TiO_2 to study the adsorption rate in degradation of MB and revealed that when increasing layer of TiO_2 to silica gel will lead to lower the adsorption rate of MB with silica gel [168].

Besides that, silica content on photocatalyst can give significant effect toward photocatalytic activity. Pu et al. [169] synthesized SiO_2/TiO_2 toward Methyl Orange (MO) degradation and from the study, increasing ratio of silica content to TiO_2 from 0 to 1/7 inhibited rutile phase which promote photocatalytic activity but excessive of silica content by 2/1 will possibly inhibited amorphous phase to anatase phase which lead to low photocatalytic activity [169]. SiO_2 composite zinc oxide via sol-gel method also showed high photocatalytic activity towards degradation of MO. The study revealed enhancement of photocatalytic activity due to the presence of SiO_2 that initiate the structure of composite to form high surface area and also produce high hydroxyl concentration [170].

5. Conclusions and recommendations for future work

Many photocatalyst have been developed and studied for wastewater treatment applications. This technology offers attractive alternative to conventional water treatment technology that can completely eliminate or destroy the emerging contaminants in wastewater. Nevertheless, there some are issues that need to be tackled to make this technology viable for wastewater treatment applications. One of the severe issues is the agglomeration of dispersed photocatalyst particle that would decrease the degradation efficiency towards pollutants due to hindrance effect. Owing to the potential application of photocatalysis in degradation of emerging contaminants, there is simple yet effective technology that has been discovered to further expand this technology and eliminates its limitations, namely integrated photocatalyst adsorbents (IPCA). This synergistic combination does not only maintain all the interesting characteristics of its individual components, but also overcomes serious drawbacks of each one, such as low absorptivity towards pollutant and rapid recombination of photogenerated electrons.

IPCA has the best potential to replace the conventional method to treat pollutants due its unique properties which involved the combination of adsorbents and photocatalysis, where the composite material had the ability to portray multiple functions. Additionally, several types of IPCA can be utilized under visible light irradiation in achieving high degradation rate of contaminants. Initial study on IPCA appears to be a promising technology for wastewater treatment and thus intensive study should be directed towards the application of IPCA on industrial pollutants and at pilot scale. There are some important things that need to be considered for industrial scale applications such as pH, temperature and recyclability. More efforts are needed to find or develop the best systems (e.g APR and FBR) to apply the IPCA as suspended solids for organic contaminants degradation. The main objectives to integrate photocatalyst with adsorbents are to enhance its photocatalytic activity. Separation with the purpose of reuse the suspension-based photocatalyst remains the main limitations for this technology. Magnetic separation has receiving numerous attractions as its offer a very convenient way for removing and recycling the magnetic particles and preventing the agglomeration and sedimentation of photocatalyst nanoparticles. Additionally, the composite can be suspended in a membrane to allow easy collection of IPCA after each treatment cycle. Thus, more efforts are needed to develop magnetic photocatalyst or composites to make this technology reliable.

Conflict of interest

None.

Acknowledgements

The authors acknowledge the financial support by the Ministry of Higher Education (MOHE) Malaysia under Grant (HiCOE) No. R.J090301.7846.4J189, R.J090301.7846.4J190 and Universiti Teknologi Malaysia (UTM). M.A. Mutalib would like to acknowledge Universiti Kebangsaan Malaysia (UKM) for PhD scholarship under the Skim Zamalah Yayasan Canselor 2016.

References

[1] T.A. Saleh, Mercury sorption by silica/carbon nanotubes and silica/activated carbon: a comparison study, J. Water Suppl.: Res. Technol. – Aqua 64 (8) (2015) 892.
[2] I. Zucker, et al., Influence of wastewater particles on ozone degradation of trace organic contaminants, Environ. Sci. Technol. 49 (1) (2015) 301–308.
[3] W. Wang, M.O. Tade, Z. Shao, Research progress of perovskite materials in photocatalysis- and photovoltaics-related energy conversion and environmental treatment, Chem. Soc. Rev. 44 (15) (2015) 5371–5408.
[4] R.K. Upadhyay, N. Soin, S.S. Roy, Role of graphene/metal oxide composites as photocatalysts, adsorbents and disinfectants in water treatment: a review, RSC Adv. 4 (8) (2014) 3823–3851.
[5] C. Qin, et al., Fabrication and visible-light photocatalytic behavior of perovskite praseodymium ferrite porous nanotubes, J. Power Sources 285 (2015) 178–184.
[6] H.-Y. Jing, et al., Efficient adsorption/photodegradation of organic pollutants from aqueous systems using Cu2O nanocrystals as a novel integrated photocatalytic adsorbent, J. Mater. Chem. A 2 (35) (2014) 14563–14570.
[7] T.A. Saleh, Nanocomposite of carbon nanotubes/silica nanoparticles and their use for adsorption of Pb (II): from surface properties to sorption mechanism, Desal. Water Treat. 57 (23) (2016) 10730–10744.
[8] N. Miranda-García, et al., Degradation study of 15 emerging contaminants at low concentration by immobilized TiO2 in a pilot plant, Catal. Today 151 (1–2) (2010)

107–113.
[9] S. Leong, et al., TiO2 based photocatalytic membranes: a review, J. Membr. Sci. 472 (2014) 167–184.
[10] F.-P. Chen, et al., Electrochemical preparation of uniform CuO/Cu2O heterojunction on beta-cyclodextrin-modified carbon fibers, J. Appl. Electrochem. 46 (3) (2016) 379–388.
[11] T.A. Saleh, Isotherm, kinetic, and thermodynamic studies on Hg (II) adsorption from aqueous solution by silica-multiwall carbon nanotubes, Environ. Sci. Pollut. Res. 22 (21) (2015) 16721–16731.
[12] T.A. Saleh, Simultaneous adsorptive desulfurization of diesel fuel over bimetallic nanoparticles loaded on activated carbon, J. Clean. Prod. 172 (2018) 2123–2132.
[13] Q. Zhu, et al., Adsorption of pyridine from aqueous solutions by polymeric adsorbents MN 200 and MN 500. Part 1: adsorption performance and PFG-NMR studies, Chem. Eng. J. 306 (2016) 67–76.
[14] A. Rahman, T. Urabe, N. Kishimoto, Color removal of reactive procion dyes by Clay adsorbents, Proc. Environ. Sci. 17 (2013) 270–278.
[15] U. Pal, et al., Mixed titanium, silicon, and aluminum oxide nanostructures as novel adsorbent for removal of rhodamine 6G and methylene blue as cationic dyes from aqueous solution, Chemosphere 163 (2016) 142–152.
[16] A. Rossner, S.A. Snyder, D.R.U. Knappe, Removal of emerging contaminants of concern by alternative adsorbents, Water Res. 43 (15) (2009) 3787–3796.
[17] C. Zhao, et al., Highly effective antifouling performance of PVDF/graphene oxide composite membrane in membrane bioreactor (MBR) system, Desalination 340 (2014) 59–66.
[18] G.K. Ramesha, et al., Graphene and graphene oxide as effective adsorbents toward anionic and cationic dyes, J. Colloid Interface Sci. 361 (1) (2011) 270–277.
[19] G.Z. Kyzas, E.A. Deliyanni, K.A. Matis, Graphene oxide and its application as an adsorbent for wastewater treatment, J. Chem. Technol. Biotechnol. 89 (2) (2014) 196–205.
[20] C. Wang, et al., Preparation of a graphene-based magnetic nanocomposite for the removal of an organic dye from aqueous solution, Chem. Eng. J. 173 (1) (2011) 92–97.
[21] T.A. Saleh, M. Tuzen, A. Sarı, Magnetic activated carbon loaded with tungsten oxide nanoparticles for aluminum removal from waters, J. Environ. Chem. Eng. 5 (3) (2017) 2853–2860.
[22] A.M. Alansi, et al., Visible-light responsive BiOBr nanoparticles loaded on reduced graphene oxide for photocatalytic degradation of dye, J. Mol. Liq. 253 (2018) 297–304.
[23] T.A. Saleh, V.K. Gupta, Photo-catalyzed degradation of hazardous dye methyl orange by use of a composite catalyst consisting of multi-walled carbon nanotubes and titanium dioxide, J. Colloid Interface Sci. 371 (1) (2012) 101–106.
[24] T.A. Saleh, V.K. Gupta, Functionalization of tungsten oxide into MWCNT and its application for sunlight-induced degradation of rhodamine B, J. Colloid Interface Sci. 362 (2) (2011) 337–344.
[25] K. Peng, et al., Perovskite LaFeO3/montmorillonite nanocomposites: synthesis, interface characteristics and enhanced photocatalytic activity, Sci. Rep. 6 (2016) 19723.
[26] K. David, et al., Photodegradation of famotidine by integrated photocatalytic adsorbent (IPCA) and kinetic study, Catal. Lett. 141 (2011) 300–308.
[27] R.A. Burns, et al., Effect of inorganic ions in heterogeneous photocatalysis of TCE, J. Environ. Eng. 125 (1) (1999) 77–85.
[28] C. Fan, et al., Fabrication of 3D CeVO4/graphene aerogels with efficient visible-light photocatalytic activity, Ceram. Int. 42 (8) (2016) 10487–10492.
[29] D. Bahnemann, D. Bockelmann, R. Goslich, Mechanistic studies of water detoxification in illuminated TiO2 suspensions, Sol. Energy Mater. 24 (1-4) (1991) 564–583.
[30] C.M. Malengreaux, et al., Study of the photocatalytic activity of Fe3+, Cr3+, La3+ and Eu3+ single-doped and co-doped TiO2 catalysts produced by aqueous sol-gel processing, J. Alloys Compd. 691 (2017) 726–738.
[31] T. Ohno, et al., Preparation of S-doped TiO 2 photocatalysts and their photocatalytic activities under visible light, Appl. Catal. A 265 (1) (2004) 115–121.
[32] J. Moon, et al., Preparation and characterization of the Sb-doped TiO2 photocatalysts, J. Mater. Sci. 36 (4) (2001) 949–955.
[33] J. Zhu, et al., Characterization of Fe–TiO 2 photocatalysts synthesized by hydrothermal method and their photocatalytic reactivity for photodegradation of XRG dye diluted in water, J. Mol. Catal. A Chem. 216 (1) (2004) 35–43.
[34] H. Wei, et al., Preparation and photocatalysis of TiO2 nanoparticles co-doped with nitrogen and lanthanum, J. Mater. Sci. 39 (4) (2004) 1305–1308.
[35] W. Zhou, et al., Preparation and properties of vanadium-doped TiO2 photocatalysts, J. Phys. D Appl. Phys. 43 (3) (2010) 035301.
[36] Q. Li, R.Z. Wen, Preparation and photocatalytic property of lanthanum-doped TiO2 nanoparticles, Advanced Materials Research, Trans Tech Publ., 2012.
[37] N. Khalid, et al., Co-doping effect of carbon and yttrium on photocatalytic activity of TiO2 nanoparticles for methyl orange degradation, J. Ovonic Res. 11 (3) (2015) 107–112.
[38] E.A. Reynoso-Soto, et al., Photocatalytic degradation of nitrobenzene using nanocrystalline TiO2 photocatalyst doped with Zn ions, J. Mex. Chem. Soc. 57 (4) (2013) 298–305.
[39] H. Yadav, et al., Enhanced visible light photocatalytic activity of Cr3+-doped anatase TiO2 nanoparticles synthesized by sol–gel method, J. Mater. Sci.: Mater. Electron. 27 (1) (2016) 526–534.
[40] O. Zuas, H. Abimanyu, W. Wibowo, Synthesis and Characterization of Nanostructured CeO, (2018).
[41] M. Khan, W. Cao, Preparation of Y-doped TiO 2 by hydrothermal method and investigation of its visible light photocatalytic activity by the degradation of methylene blue, J. Mol. Catal. A Chem. 376 (2013) 71–77.
[42] J. Sun, et al., Photocatalytic degradation of Orange G on nitrogen-doped TiO 2 catalysts under visible light and sunlight irradiation, J. Hazard. Mater. 155 (1) (2008) 312–319.
[43] T. Ohno, et al., Preparation of S-doped TiO2 photocatalysts and their photocatalytic activities under visible light, Appl. Catal. A 265 (1) (2004) 115–121.
[44] C.J. Brinker, G.W. Scherer, Sol-Gel Science: the Physics and Chemistry of sol-Gel Processing, Academic press, 2013.
[45] J. Zhu, et al., Hydrothermal doping method for preparation of Cr 3+-TiO 2 photocatalysts with concentration gradient distribution of Cr 3+, Appl. Catal. B: Environ. 62 (3) (2006) 329–335.
[46] Y.-T. Lin, et al., Effect of C content and calcination temperature on the photocatalytic activity of C-doped TiO 2 catalyst, Sep. Purif. Technol. 116 (2013) 114–123.
[47] C.M. Malengreaux, et al., Study of the photocatalytic activity of Fe 3+, Cr 3+, La 3+ and Eu 3+ single-doped and co-doped TiO 2 catalysts produced by aqueous sol-gel processing, J. Alloys Compd. 691 (2017) 726–738.
[48] S. Song, et al., Influences of pH value in deposition-precipitation synthesis process on Pt-doped TiO 2 catalysts for photocatalytic oxidation of NO, J. Environ. Sci. 24 (8) (2012) 1519–1524.
[49] J. Shi, L. Guo, ABO3-based photocatalysts for water splitting, Prog. Nat. Sci.: Mater. Int. 22 (6) (2012) 592–615.
[50] S. Thirumalairajan, et al., Controlled synthesis of perovskite LaFeO3 microsphere composed of nanoparticles via self-assembly process and their associated photocatalytic activity, Chem. Eng. J. 209 (2012) 420–428.
[51] M. Abd Mutalib, et al., Progress towards highly stable and lead-free perovskite solar cells, Mater. For. Renew. Sustain. Energy 7 (2) (2018) 7.
[52] H. Li, B. Feng, Visible-light-driven composite La2O3/TiO2 nanotube arrays: synthesis and improved photocatalytic activity, Mater. Sci. Semicond. Process. 43 (2016) 55–59.
[53] M.A. Mutalib, et al., Enhancement in photocatalytic degradation of methylene blue by LaFeO3-GO integrated photocatalyst-adsorbents under visible light irradiation, Korean J. Chem. Eng. 35 (2) (2018) 548–556.
[54] W. Wu, et al., Synthesis, structures and photocatalytic activities of microcrystalline ABi2Nb2O9 (A = Sr, Ba) powders, J. Solid State Chem. 184 (1) (2011) 81–88.
[55] S. Basha, et al., On the adsorption/photodegradation of amoxicillin in aqueous solutions by an integrated photocatalytic adsorbent (IPCA): experimental studies and kinetics analysis, Photochem. Photobiol. Sci. 10 (6) (2011) 1014–1022.
[56] T.-D. Nguyen-Phan, et al., Mesoporous titanosilicate/reduced graphene oxide composites: layered structure, high surface-to-volume ratio, doping effect and application in dye removal from water, J. Mater. Chem. 22 (38) (2012) 20504–20511.
[57] A. Rapsomanikis, et al., Nanocrystalline TiO2 and halloysite clay mineral composite films prepared by sol-gel method: synergistic effect and the case of silver modification to the photocatalytic degradation of basic blue-41 Azo dye in water, Glob. Nest J. 16 (3) (2014) 485–498.
[58] F. Haque, et al., Preparation and performance of integrated photocatalyst adsorbent (IPCA) employed to degrade model organic compounds in synthetic wastewater, J. Photochem. Photobiol. A Chem. 169 (1) (2005) 21–27.
[59] Y. Liu, et al., Novel visible light-induced g-C3N4–Sb2S3/Sb4O5Cl2 composite photocatalysts for efficient degradation of methyl orange, Catal. Commun. 70 (2015) 17–20.
[60] T. Sun, et al., Ag/g-C3N4 photocatalysts: microwave-assisted synthesis and enhanced visible-light photocatalytic activity, Catal. Commun. 79 (2016) 45–48.
[61] Y. Huang, et al., Synthesis of AgCl/Bi3O4Cl composite and its photocatalytic activity in RhB degradation under visible light, Catal. Commun. 76 (2016) 19–22.
[62] S. Ning, et al., One-pot fabrication of Bi3O4Cl/BiOCl plate-on-plate heterojunction with enhanced visible-light photocatalytic activity, Appl. Catal. B: Environ. 185 (2016) 203–212.
[63] X. Lin, et al., Photocatalytic activity of a Bi-based oxychloride Bi3O4Cl, J. Phys. Chem. B 110 (48) (2006) 24629–24634.
[64] S. Pourbeyram, Effective removal of heavy metals from aqueous solutions by graphene oxide–zirconium phosphate (GO–Zr-P) nanocomposite, Ind. Eng. Chem. Res. 55 (19) (2016) 5608–5617.
[65] Y. Yu, X. Li, J. Cheng, A comparison study of mechanism: Cu2+ adsorption on different adsorbents and their surface-modified adsorbents, J. Chem. 2016 (2016) 8.
[66] T.A. Saleh, M.M. Al-Shalalfeh, A.A. Al-Saadi, Silver nanoparticles for detection of methimazole by surface-enhanced Raman spectroscopy, Mater. Res. Bull. 91 (2017) 173–178.
[67] M.M. Al-Shalalfeh, et al., Spherical silver nanoparticles as substrates in surface-enhanced Raman spectroscopy for enhanced characterization of ketoconazole, Mater. Sci. Eng. C 76 (2017) 356–364.
[68] N. Tka, et al., Amines modified fibers obtained from natural Populus tremula and their rapid biosorption of acid blue 25, J. Mol. Liq. 250 (2018) 423–432.
[69] S.A. Hassanzadeh-Tabrizi, M.M. Motlagh, S. Salahshour, Synthesis of ZnO/CuO nanocomposite immobilized on γ-Al2O3 and application for removal of methyl orange, Appl. Surf. Sci. 384 (2016) 237–243.
[70] L. Wu, et al., Removal of uranium and fluorine from wastewater by double-functional microsphere adsorbent of SA/CMC loaded with calcium and aluminum, Appl. Surf. Sci. 384 (2016) 466–479.
[71] W. Qiu, et al., Efficient removal of Cr(VI) by magnetically separable CoFe2O4/activated carbon composite, J. Alloys Compd. 678 (2016) 179–184.
[72] G. Ersan, et al., Adsorption of organic contaminants by graphene nanosheets, carbon nanotubes and granular activated carbons under natural organic matter preloading conditions, Sci. Total Environ. 565 (2016) 811–817.
[73] H.A. Hegazi, Removal of heavy metals from wastewater using agricultural and

industrial wastes as adsorbents, HBRC J. 9 (3) (2013) 276–282.
[74] M.E. Fernandez, et al., Development and characterization of activated hydrochars from orange peels as potential adsorbents for emerging organic contaminants, Bioresour. Technol. 183 (2015) 221–228.
[75] M. Liu, et al., Magnetically separable Ag/AgCl-zero valent iron particles modified zeolite X heterogeneous photocatalysts for tetracycline degradation under visible light, Chem. Eng. J. 302 (2016) 475–484.
[76] F. Macht, et al., Specific surface area of clay minerals: comparison between atomic force microscopy measurements and bulk-gas (N2) and -liquid (EGME) adsorption methods, Appl. Clay Sci. 53 (1) (2011) 20–26.
[77] A.J. Fletcher, Y. Uygur, K.M. Thomas, Role of surface functional groups in the adsorption kinetics of water vapor on microporous activated carbons, J. Phys. Chem. C 111 (23) (2007) 8349–8359.
[78] A. Nasrollahpour, S.E. Moradi, Photochemical degradation of methylene blue by metal oxide-supported activated carbon photocatalyst, Desal. Water Treat. 57 (19) (2016) 8854–8862.
[79] V. Vimonses, et al., An adsorption–photocatalysis hybrid process using multi-functional-nanoporous materials for wastewater reclamation, Water Res. 44 (18) (2010) 5385–5397.
[80] M.N. Chong, et al., Optimisation of an annular photoreactor process for degradation of Congo Red using a newly synthesized titania impregnated kaolinite nano-photocatalyst, Sep. Purif. Technol. 67 (3) (2009) 355–363.
[81] W. Zhang, L. Zou, L. Wang, Photocatalytic TiO2/adsorbent nanocomposites prepared via wet chemical impregnation for wastewater treatment: a review, Appl. Catal. A 371 (1–2) (2009) 1–9.
[82] D. Kanakaraju, et al., Titanium dioxide/zeolite integrated photocatalytic adsorbents for the degradation of amoxicillin, Appl. Catal. B: Environ. 166–167 (2015) 45–55.
[83] S. Gomez, et al., In situ generated TiO2 over zeolitic supports as reusable photocatalysts for the degradation of dichlorvos, Appl. Catal. B: Environ. 162 (2015) 167–173.
[84] O.E. Jaime-Acuña, et al., Disperse orange 30 dye degradation by assisted plasmonic photocatalysis using Ag-CdZnSO/zeolitic matrix nanocomposites, Catal. Commun. 75 (2016) 103–107.
[85] N.F. Zainudin, A.Z. Abdullah, A.R. Mohamed, Characteristics of supported nano-TiO2/ZSM-5/silica gel (SNTZS): photocatalytic degradation of phenol, J. Hazard. Mater. 174 (1–3) (2010) 299–306.
[86] M. Khatamian, S. Hashemian, S. Sabaee, Preparation and photo-catalytic activity of nano-TiO2–ZSM-5 composite, Mater. Sci. Semicond. Process. 13 (3) (2010) 156–161.
[87] A.N. Ökte, Ö. Yılmaz, Characteristics of lanthanum loaded TiO2-ZSM-5 photocatalysts: decolorization and degradation processes of methyl orange, Appl. Catal. A 354 (1–2) (2009) 132–142.
[88] A. Neren Ökte, Ö. Yılmaz, Photodecolorization of methyl orange by yttrium incorporated TiO2 supported ZSM-5, Appl. Catal. B: Environ. 85 (1–2) (2008) 92–102.
[89] C. Zhao, et al., Advantages of TiO2/5A composite catalyst for photocatalytic degradation of antibiotic oxytetracycline in aqueous solution: comparison between TiO2 and TiO2/5A composite system, Chem. Eng. J. 248 (2014) 280–289.
[90] Y. Chen, K. Liu, Preparation and characterization of nitrogen-doped TiO2/diatomite integrated photocatalytic pellet for the adsorption-degradation of tetracycline hydrochloride using visible light, Chem. Eng. J. 302 (2016) 682–696.
[91] Q. Zhang, et al., TiO2 nanotube-carbon macroscopic monoliths with multimodal porosity as efficient recyclable photocatalytic adsorbents for water purification, Mater. Chem. Phys. 173 (2016) 452–459.
[92] M. Akkari, et al., ZnO/clay nanoarchitectures: synthesis, characterization and evaluation as photocatalysts, Appl. Clay Sci. 131 (2016) 131–139.
[93] S. Vadivel, et al., Graphene oxide–BiOBr composite material as highly efficient photocatalyst for degradation of methylene blue and rhodamine-B dyes, J. Water Process Eng. 1 (2014) 17–26.
[94] S. Bera, et al., Hierarchically structured ZnO-graphene hollow microspheres towards effective reusable adsorbent for organic pollutant via photodegradation process, J. Alloys Compd. 669 (2016) 177–186.
[95] S. Basha, et al., Studies on the adsorption and kinetics of photodegradation of pharmaceutical compound, indomethacin using novel photocatalytic adsorbents (IPCAs), Ind. Eng. Chem. Res. 49 (22) (2010) 11302–11309.
[96] J.G. McEvoy, Z. Zhang, Synthesis and characterization of Ag/AgBr-activated carbon composites for visible light induced photocatalytic detoxification and disinfection, J. Photochem. Photobiol. A Chem. 321 (2016) 161–170.
[97] T. Kamal, et al., Adsorption and photocatalyst assisted dye removal and bactericidal performance of ZnO/chitosan coating layer, Int. J. Biol. Macromol. 81 (2015) 584–590.
[98] S. Wang, S. Zhou, Photodegradation of methyl orange by photocatalyst of CNTs/P-TiO2 under UV and visible-light irradiation, J. Hazard. Mater. 185 (1) (2011) 77–85.
[99] M. Ahmad, et al., Graphene–Ag/ZnO nanocomposites as high performance photocatalysts under visible light irradiation, J. Alloys Compd. 577 (2013) 717–727.
[100] T. Nakajima, et al., Combined use of photocatalyst and adsorbent for the removal of inorganic arsenic(III) and organoarsenic compounds from aqueous media, J. Hazard. Mater. 120 (1–3) (2005) 75–80.
[101] M. Zhang, et al., Separation free C3N4/SiO2 hybrid hydrogels as high active photocatalysts for TOC removal, Appl. Catal. B: Environ. 194 (2016) 105–110.
[102] S. Sohrabnezhad, A. Pourahmad, M. Razavi, Silver bromide in montmorillonite as visible light-driven photocatalyst and the role of montmorillonite, Appl. Phys. A: Mater. Sci. Proces. 122 (9) (2016).
[103] F. Fresno, et al., Photocatalytic materials: recent achievements and near future trends, J. Mater. Chem. A 2 (9) (2014) 2863–2884.
[104] J.C. Colmenares, P. Lisowski, D. Lomot, A novel biomass-based support (Starbon) for TiO2 hybrid photocatalysts: a versatile green tool for water purification, RSC Adv. 3 (43) (2013) 20186–20192.
[105] T.S. Anirudhan, F. Shainy, J. Christa, Synthesis and characterization of polyacrylic acid- grafted-carboxylic graphene/titanium nanotube composite for the effective removal of enrofloxacin from aqueous solutions: adsorption and photocatalytic degradation studies, J. Hazard. Mater. 324 (Part B) (2017) 117–130.
[106] D. Liu, et al., Porous BN/TiO2 hybrid nanosheets as highly efficient visible-light-driven photocatalysts, Appl. Catal. B: Environ. 207 (2017) 72–78.
[107] M. Aliofkhazraei, et al., Graphene Science Handbook: Size-Dependent Properties, CRC Press, 2016.
[108] P. Pucher, et al., A photocatalytic active adsorbent for gas cleaning in a fixed bed reactor, Int. J. Photoenergy 2008 (2008) 7.
[109] Y. Zhang, Z. Nan, Preparation of magnetic ZnLa0.02Fe1.98O4/MWCNTs composites and investigation on its adsorption of methyl orange from aqueous solution, Mater. Res. Bull. 66 (2015) 176–185.
[110] Y. Shao, et al., Application of Mn/MCM-41 as an adsorbent to remove methyl blue from aqueous solution, J. Colloid Interface Sci. 429 (2014) 25–33.
[111] A. Taufik, R. Saleh, Synergistic effect between ternary iron–zinc–copper mixed oxides and graphene for photocatalytic water decontamination, Ceram. Int. 43 (4) (2017) 3510–3520.
[112] N. Tafreshi, S. Sharifnia, S. Moradi Dehaghi, Box–Behnken experimental design for optimization of ammonia photocatalytic degradation by ZnO/Oak charcoal composite, Process Saf. Environ. Prot. 106 (2017) 203–210.
[113] F. Chen, et al., Construction of rGO/Fe3O4/Ag3PO4 multifunctional composite as recyclable adsorbent and photocatalysts towards the mixture of dyes in water under visible light irradiation, Mater. Lett. 185 (2016) 561–564.
[114] L.F. Velasco, J.B. Parra, C.O. Ania, Role of activated carbon features on the photocatalytic degradation of phenol, Appl. Surf. Sci. 256 (17) (2010) 5254–5258.
[115] N. Linares, et al., Mesoporous materials for clean energy technologies, Chem. Soc. Rev. 43 (22) (2014) 7681–7717.
[116] X.-W. Wu, et al., Adsorption properties and mechanism of mesoporous adsorbents prepared with fly ash for removal of Cu(II) in aqueous solution, Appl. Surf. Sci. 261 (2012) 902–907.
[117] A.M. Busuioc, et al., Growth of anatase nanoparticles inside the mesopores of SBA-15 for photocatalytic applications, Catal. Commun. 8 (3) (2007) 527–530.
[118] G.L. Puma, et al., Preparation of titanium dioxide photocatalyst loaded onto activated carbon support using chemical vapor deposition: a review paper, J. Hazard. Mater. 157 (2) (2008) 209–219.
[119] D. Huang, et al., A new method to prepare high-surface-area N–TiO 2/activated carbon, Mater. Lett. 65 (2) (2011) 326–328.
[120] H. Wang, et al., High photocatalytic degradation of tetracycline under visible light with Ag/AgCl/activated carbon composite plasmonic photocatalyst, J. Ind. Eng. Chem. 35 (2016) 83–92.
[121] J.G. McEvoy, W. Cui, Z. Zhang, Synthesis and characterization of Ag/AgCl–activated carbon composites for enhanced visible light photocatalysis, Appl. Catal. B: Environ. 144 (2014) 702–712.
[122] J.G. McEvoy, et al., Visible-light-driven inactivation of Escherichia coli K-12 using an Ag/AgCl–activated carbon composite photocatalyst, J. Photochem. Photobiol. A Chem. 267 (2013) 25–34.
[123] P. Muthirulan, M. Meenakshisundararam, N. Kannan, Beneficial role of ZnO photocatalyst supported with porous activated carbon for the mineralization of alizarin cyanin green dye in aqueous solution, J. Adv. Res. 4 (6) (2013) 479–484.
[124] C. Wang, et al., Preparation, characterization and photocatalytic activity of a novel composite photocatalyst: ceria-coated activated carbon, J. Hazard. Mater. 184 (1) (2010) 1–5.
[125] X. Lu, et al., Characterization and photocatalytic activity of Zn 2+–TiO 2/AC composite photocatalyst, Appl. Surf. Sci. 258 (5) (2011) 1656–1661.
[126] J. Xu, et al., Synthesis of fluorine-doped titania-coated activated carbon under low temperature with high photocatalytic activity under visible light, J. Phys. Chem. Solids 69 (10) (2008) 2366–2370.
[127] J.-h. Sun, et al., Photodegradation of azo dye Congo Red from aqueous solution by the WO 3–TiO 2/activated carbon (AC) photocatalyst under the UV irradiation, Mater. Chem. Phys. 115 (1) (2009) 303–308.
[128] X. Zhang, M. Zhou, L. Lei, Preparation of an Ag–TiO 2 photocatalyst coated on activated carbon by MOCVD, Mater. Chem. Phys. 91 (1) (2005) 73–79.
[129] Y. Ao, et al., Magnetically separable composite photocatalyst with enhanced photocatalytic activity, J. Hazard. Mater. 160 (2) (2008) 295–300.
[130] J.-w. Shi, Preparation of Fe (III) and Ho (III) co-doped TiO 2 films loaded on activated carbon fibers and their photocatalytic activities, Chem. Eng. J. 151 (1) (2009) 241–246.
[131] H. Choi, E. Stathatos, D.D. Dionysiou, Sol–gel preparation of mesoporous photocatalytic TiO 2 films and TiO 2/Al 2 O 3 composite membranes for environmental applications, Appl. Catal. B: Environ. 63 (1) (2006) 60–67.
[132] B. Tryba, Increase of the photocatalytic activity of TiO, Int. J. Photoenergy 2008 (2008).
[133] S. Liu, X. Chen, Preparation and characterization of a novel activated carbon--supported N-doped visible light response photocatalyst (TiO2− xNy/AC), J. Chem. Technol. Biotechnol. 82 (5) (2007) 453–459.
[134] A.H. El-Sheikh, et al., Oxidized activated carbon as support for titanium dioxide in UV-assisted degradation of 3-chlorophenol, Sep. Purif. Technol. 54 (1) (2007) 117–123.
[135] S. Sohrabnezhad, M. Zanjanchi, M. Razavi, Plasmon-assisted degradation of methylene blue with Ag/AgCl/montmorillonite nanocomposite under visible light, Spectrochim. Acta, Part A 130 (2014) 129–135.

[136] W. Qiu, et al., Efficient removal of Cr (VI) by magnetically separable CoFe 2 O 4/ activated carbon composite, J. Alloys Compd. 678 (2016) 179–184.
[137] H. Yang, P. Fu, Surface properties and catalytic performance of activated carbon fibers supported TiO 2 photocatalyst, Surf. Rev. Lett. 15 (04) (2008) 337–344.
[138] A. Ramesh, et al., Adsorption of inorganic and organic arsenic from aqueous solutions by polymeric Al/Fe modified montmorillonite, Sep. Purif. Technol. 56 (1) (2007) 90–100.
[139] A. Sdiri, et al., Evaluating the adsorptive capacity of montmorillonitic and calcareous clays on the removal of several heavy metals in aqueous systems, Chem. Eng. J. 172 (1) (2011) 37–46.
[140] H. Xu, et al., Quantum sized zinc oxide immobilized on bentonite clay and degradation of CI acid Red 35 in aqueous under ultraviolet light, Int. J. Photoenergy 2015 (2015).
[141] L. Bouna, B. Rhouta, F. Maury, Physicochemical study of photocatalytic activity of TiO2 supported palygorskite clay mineral, Int. J. Photoenergy 2013 (2013).
[142] J.-M. Herrmann, Heterogeneous photocatalysis: fundamentals and applications to the removal of various types of aqueous pollutants, Catal. Today 53 (1) (1999) 115–129.
[143] C. Belver, J. Bedia, J.J. Rodriguez, Zr-doped TiO_2 supported on delaminated clay materials for solar photocatalytic treatment of emerging pollutants, J. Hazard. Mater. 322 (2017) 233–242.
[144] W. Lutz, Y. Zeolite, Synthesis, modification, and Properties— A case revisited, Adv. Mater. Sci. Eng. 2014 (2014) 20.
[145] K. Guesh, et al., Enhanced photocatalytic activity of TiO2 supported on zeolites tested in real wastewaters from the textile industry of Ethiopia, Microporous Mesoporous Mater. 225 (2016) 88–97.
[146] M. Takeuchi, et al., Enhancement of the photocatalytic reactivity of TiO2 nanoparticles by a simple mechanical blending with hydrophobic mordenite (MOR) zeolite, Appl. Catal. B: Environ. 89 (3-4) (2009) 406–410.
[147] T. Kamegawa, et al., Design of TiO2-zeolite composites with enhanced photocatalytic performances under irradiation of UV and visible light, Microporous Mesoporous Mater. 165 (2013) 142–147.
[148] M.S. Dresselhaus, G. Dresselhaus, Intercalation compounds of graphite, Adv. Phys. 51 (1) (2002) 1–186.
[149] M.J. Allen, V.C. Tung, R.B. Kaner, Honeycomb carbon: a review of graphene, Chem. Rev. 110 (1) (2010) 132–145.
[150] Q. Xiang, J. Yu, M. Jaroniec, Graphene-based semiconductor photocatalysts, Chem. Soc. Rev. 41 (2) (2012) 782–796.
[151] M.D. Stoller, et al., Graphene-based ultracapacitors, Nano Lett. 8 (10) (2008) 3498–3502.
[152] P. Wang, et al., Synthesis of reduced graphene oxide-anatase TiO2 nanocomposite and its improved photo-induced charge transfer properties, Nanoscale 3 (4) (2011) 1640–1645.
[153] I.V. Lightcap, T.H. Kosel, P.V. Kamat, Anchoring semiconductor and metal nanoparticles on a two-dimensional catalyst mat. Storing and shuttling electrons with reduced graphene oxide, Nano Lett. 10 (2) (2010) 577–583.
[154] P.V. Kamat, Graphene-based nanoassemblies for energy conversion, J. Phys. Chem. Lett. 2 (3) (2011) 242–251.
[155] Y.-E. Moon, et al., Poly (vinyl alcohol)/poly (acrylic acid)/TiO 2/graphene oxide nanocomposite hydrogels for pH-sensitive photocatalytic degradation of organic pollutants, Mater. Sci. Eng. B 178 (17) (2013) 1097–1103.
[156] N. Yahya, et al., Adsorption and photocatalytic study of integrated photocatalyst adsorbent (IPCA) using LaFeO3-GO nanocomposites for removal of synthetic dyes, Chem. Eng. Trans. 63 (2018) 517–522.
[157] D.-H. Yoo, et al., Enhanced photocatalytic activity of graphene oxide decorated on TiO 2 films under UV and visible irradiation, Curr. Appl. Phys. 11 (3) (2011) 805–808.
[158] J. Lee, et al., New series connection method for bulk-heterojunction polymer solar cell modules, Sol. Energy Mater. Sol. Cells 98 (0) (2012) 208–211.
[159] N.S. Alim, H.O. Lintang, L. Yuliati, Improved photocatalytic activity of anatase titanium dioxide by reduced graphene oxide, Malaysian J. Fundam. Appl. Sci. 11 (3) (2015).
[160] N.A. Zubir, Graphene Oxide-Iron Oxide Nanocomposites for Dye Contaminated Wastewater Remediation, (2015).
[161] A. Bhatnagar, M. Sillanpää, Applications of chitin- and chitosan-derivatives for the detoxification of water and wastewater - a short review, Adv. Colloid Interface Sci. 152 (1–2) (2009) 26–38.
[162] Y. Ren, et al., Magnetic EDTA-modified chitosan/SiO2/Fe3O4 adsorbent: preparation, characterization, and application in heavy metal adsorption, Chem. Eng. J. 226 (2013) 300–311.
[163] Y. Peng, et al., Chitosan-modified palygorskite: preparation, characterization and reactive dye removal, Appl. Clay Sci. 74 (2013) 81–86.
[164] G. Crini, P.M. Badot, Application of chitosan, a natural aminopolysaccharide, for dye removal from aqueous solutions by adsorption processes using batch studies: a review of recent literature, Prog. Polym. Sci. (Oxf.) 33 (4) (2008) 399–447.
[165] N. Ngadi, et al., Removal of ethyl orange dye using hybrid chitosan and zinc oxide, J. Teknol. 67 (1) (2014).
[166] Y. Haldorai, J.-J. Shim, Multifunctional chitosan-copper oxide hybrid material: photocatalytic and antibacterial activities, Int. J. Photoenergy 2013 (2013) 8.
[167] Z. Zainal, et al., Characterization of TiO 2–Chitosan/Glass photocatalyst for the removal of a monoazo dye via photodegradation–adsorption process, J. Hazard. Mater. 164 (1) (2009) 138–145.
[168] Y.M. Wang, et al., Preparation and photocatalytic properties of silica gel-supported TiO 2, Mater. Lett. 60 (7) (2006) 974–978.
[169] Y. Pu, et al., Microemulsion synthesis of nanosized SiO2/TiO2 particles and their photocatalytic activity, Chin. J. Catal. 28 (3) (2007) 251–256.
[170] J.B. Zhong, et al., Fabrication and catalytic performance of SiO2-ZnO composite photocatalyst, Synth. React. Inorg., Metal-Org., Nano-Metal Chem. 44 (8) (2014) 1203–1207.